Erschienen in: Cell chemical biology ; 27 (2020), 12. - S. 1510-1520.e6
https://dx.doi.org/10.1016/j.chembiol.2020.08.017

Identification of Small-Molecule Activators of the Ubiquitin Ligase E6AP/UBE3A and Angelman Syndrome-Derived E6AP/UBE3A Variants

Fabian Offensperger,[1,3] Franziska Müller,[1] Jasmin Jansen,[1,3] Daniel Hammler,[2,3] Kathrin H. Götz,[2,3] Andreas Marx,[2,3] Carissa L. Sirois,[4] Stormy J. Chamberlain,[4] Florian Stengel,[1,3] and Martin Scheffner[1,3,5,*]

[1]Department of Biology, University of Konstanz, Konstanz, Germany
[2]Department of Chemistry, University of Konstanz, Konstanz, Germany
[3]Konstanz Research School Chemical Biology, University of Konstanz, Konstanz, Germany
[4]Department of Genetics and Genome Sciences, UConn Health, University of Connecticut, Farmington, CT, USA
[5]Lead Contact
*Correspondence: martin.scheffner@uni-konstanz.de

SUMMARY

Genetic aberrations of the *UBE3A* gene encoding the E3 ubiquitin ligase E6AP underlie the development of Angelman syndrome (AS). Approximately 10% of AS individuals harbor *UBE3A* genes with point mutations, frequently resulting in the expression of full-length E6AP variants with defective E3 activity. Since E6AP exists in two states, an inactive and an active one, we hypothesized that distinct small molecules can stabilize the active state and that such molecules may rescue the E3 activity of AS-derived E6AP variants. Therefore, we established an assay that allows identifying modulators of E6AP in a high-throughput format. We identified several compounds that not only stimulate wild-type E6AP but also rescue the E3 activity of certain E6AP variants. Moreover, by chemical cross-linking coupled to mass spectrometry we provide evidence that the compounds stabilize an active conformation of E6AP. Thus, these compounds represent potential lead structures for the design of drugs for AS treatment.

INTRODUCTION

The ubiquitin ligase E6AP, the founding member of the HECT family of E3 ubiquitin ligases (Huibregtse et al., 1995; Scheffner et al., 1995), was originally identified as a protein that is recruited by the E6 oncoprotein of cancer-associated human papillomaviruses (HPVs) to target the tumor suppressor p53 for ubiquitination and degradation by the proteasome (Huibregtse et al., 1993; Scheffner et al., 1993). Remarkably, later studies revealed that deregulation of E6AP is critically involved not only in HPV-induced cervical carcinogenesis, but also in the development of distinct neurodevelopmental disorders. E6AP is encoded by the *UBE3A* gene located on chromosome 15q11–13 (Sutcliffe et al., 1997; Yamamoto et al., 1997). While genetic alterations of the *UBE3A* gene resulting in loss of E6AP expression or in the expression of E6AP variants with compromised E3 activity are the cause of the Angelman syndrome (AS), amplification of the chromosomal region containing the *UBE3A* gene is found in individuals with Dup15q syndrome, an autism spectrum disorder (Buiting et al., 2016; Dagli et al., 2012; Glessner et al., 2009; Hogart et al., 2010; Khatri and Man, 2019; Kishino et al., 1997; LaSalle et al., 2015; Matsuura et al., 1997). Thus, E6AP represents an impressive example of the notion that dysregulation of ubiquitination plays an important role in the development of human disease.

To obtain insight into how dysregulation of E6AP contributes to the development of different disorders, the identification of respective substrate proteins of E6AP appears to be most relevant. For cervical cancer, several substrates of the E6-E6AP complex, including p53 and distinct PDZ domain-containing proteins, have been identified (for reviews, see Wallace and Galloway, 2015; White and Howley, 2013). Although the list of substrates may not be complete yet, the unscheduled degradation of these is likely to contribute to HPV-induced carcinogenesis. Similarly, a number of proteins have been reported to serve as potential substrates for E6AP also in the absence of the viral E6 oncoprotein, including HHR23A and HHR23B, alpha-Synuclein, Ring1B, Ephexin-5, and, most recently, BK channels (Kumar et al., 1999; Margolis et al., 2010; Mulherkar et al., 2009; Sun et al., 2019; Zaaroor-Regev et al., 2010). Although the importance of the ability of E6AP to target these proteins for AS and/or Dup15q syndrome remains to be determined, it is tempting to speculate that at least some of the E6AP substrates are relevant for both disorders. Another important issue is the identification of processes and mechanisms that regulate E6AP activity. In a simplified view, the activity of E6AP can be controlled at the level of expression and/or posttranslationally at the level of its enzymatic function. Indeed, the paternal *UBE3A* allele is silenced in certain brain areas by a long non-coding RNA (Hsiao et al., 2019; Rougeulle et al., 1997; Runte et al., 2001). Furthermore, in approximately 75% of AS individuals the functional

maternal allele is lost, resulting in significantly reduced E6AP expression levels, while individuals with Dup15q syndrome harbor an additional *UBE3A* allele potentially resulting in increased E6AP levels. In addition, the *UBE3A* gene encodes three isoforms that differ in their very N-terminal regions (Yamamoto et al., 1997), and it was recently reported that the shortest isoform in mice, which corresponds to human isoform 1, localizes to the nucleus and that loss of nuclear localization is associated with AS development (Avagliano Trezza et al., 2019).

The above data indicate that, at least in certain brain areas, E6AP expression and subcellular localization have to be tightly controlled for proper development. However, there is also increasing evidence that the enzymatic activity of E6AP is subject to regulation. The phosphorylation status of T485 (numbering according to isoform 1; Yamamoto et al., 1997) affects E6AP activity, and a respective mutation that results in increased E6AP activity has been found in an individual with autism spectrum disorder (Yi et al., 2015). Furthermore, we reported that E6AP can be allosterically activated by the HPV E6 oncoprotein (Mortensen et al., 2015) and by HERC2 (Kühnle et al., 2011), a member of the HECT E3 family, which has been causally associated with a neurodevelopmental syndrome with AS-like features (Harlalka et al., 2013). Based on these data, we hypothesized that E6AP exists in at least two different conformational states. However, while the structure of the catalytic HECT domain was solved 2 decades ago (Huang et al., 1999), information about the structure of full-length E6AP or even the N-terminal part of E6AP—with the exception of the AZUL domain and the E6 binding region (Lemak et al., 2011; Martinez-Zapien et al., 2016)—is missing. Nonetheless, by using a cross-linking coupled to mass spectrometry (XL-MS) approach, we recently showed that binding of the E6 oncoprotein induces conformational rearrangements in E6AP, presumably stabilizing an enzymatically active state of E6AP (Sailer et al., 2018).

The fact that unscheduled activation as well as inactivation of E6AP contributes to the development of distinct human disorders makes E6AP an attractive target for therapeutic approaches. We, therefore, developed a fluorescence polarization (FP)-based approach to monitor E3-mediated ubiquitination that is suitable for high-throughput screening in order to identify small-molecule modulators of E6AP or other E3 ubiquitin ligases. By this approach, we identified several compounds that stimulate E6AP activity in a selective manner. Moreover, some of these compounds, as well as the E6 oncoprotein, rescue the E3 activity of a distinct set of E6AP variants derived from AS individuals. Finally, we show that, similar to the E6 oncoprotein, these compounds induce structural rearrangements in E6AP and AS-derived E6AP variants, stabilizing an enzymatically active state. Thus, these compounds represent potential lead structures for the design of small-molecule activators of E6AP that can be employed for analyzing E6AP activity in cells and as potential therapeutics.

RESULTS

A Fluorescence Polarization-Based Ubiquitination Assay to Monitor E6AP Activity

The principle of the FP-based assay to measure E6AP activity (Figure 1A) is based on the facts that (1) due to Brownian motion, smaller molecules such as free ubiquitin tumble faster than larger ones such as ubiquitin-protein conjugates, and (2) FP is a well-established method to monitor such differences in tumbling speed (Hall et al., 2016; Huang and Aulabaugh, 2016). To measure ubiquitination by FP, we labeled ubiquitin with the fluorescent dye TAMRA via NHS coupling by adaptation of a procedure that results in site-specific modification of ubiquitin with biotin at K6 (Shang et al., 2005). Indeed, liquid chromatography and mass spectrometric analysis of TAMRA-labeled ubiquitin showed that under the conditions used, ubiquitin is mainly modified with one TAMRA molecule (Ub-T) and that this preferably occurs at K6 (Figure S1).

A common feature of many E3 ligases, including E6AP, is that they can ubiquitinate themselves (auto-ubiquitination) (Nuber et al., 1998; Zheng and Shabek, 2017). Thus, to determine if E6AP can use Ub-T for ubiquitination (note that E6AP mainly generates K48-linked ubiquitin chains; Kim and Huibregtse, 2009; Wang and Pickart, 2005) and if this can be measured by FP, we performed E6AP auto-ubiquitination assays. To do so, we incubated increasing concentrations of bacterially expressed E6AP with the E1-ubiquitin-activating enzyme, a cognate E2-ubiquitin-conjugating enzyme (UbcH5b or UbcH7), and a mixture consisting of Ub-T and non-modified ubiquitin (1:10 ratio) in the absence and presence of the E6 oncoprotein. The reactions were stopped at different times and analyzed either by FP (Figure 1B) or by FP and SDS-PAGE followed by fluorescence readout (Figure 1C). This showed that Ub-T is used by E6AP for auto-ubiquitination and that this process can be readily monitored by FP. In detail, in the absence of ATP, E1, or E2, the FP value stays at approximately 180 mP, which reflects the value for free Ub-T, and this value does not change over time. In the presence of ATP, E1, and E2, but in absence of E6AP, the FP value is also approximately 180 mP, while it can reach values up to 280 mP in the presence of E6AP (Figures 1C and S1). Since an increase is not observed with a catalytically inactive E6AP mutant (E6AP_C820A; Figure 1B), this demonstrates that the increase in FP values depends on E6AP auto-ubiquitination. Notably, the FP-based assay is not limited to E6AP, but can also be used to monitor the activity of other E3s (Figure S1), including members of the RING E3 family and the HECT E3 family, as shown for HDM2 and truncated forms of RLIM and HUWE1 (Adhikary et al., 2005; Honda et al., 1997; Ostendorff et al., 2002).

Taken together, the results show that the FP-based ubiquitination assay is a suitable approach to follow the progress of a ubiquitination reaction in a time-resolved manner. Furthermore, the dynamic range of the observed FP values results in Z′ values of $\geq$0.8 (Figure S2C), indicating that the assay is well suited to identify modulators of E6AP activity in a high-throughput screening format (Zhang et al., 1999). In fact, by adjusting the concentration of E6AP, the FP-based auto-ubiquitination assay can be employed to identify activators of E6AP—as exemplified by the stimulatory effect of the E6 protein, when using limiting amounts of E6AP (Figures 1B and 1C)—as well as inhibitors, when using higher amounts of E6AP (Figure 1B).

Screening for Small-Molecule Activators of E6AP

Since the E6 oncoprotein acts as an allosteric activator of E6AP (Mortensen et al., 2015), we reasoned that such an allosteric effect should also be achievable by small molecules. Therefore, we

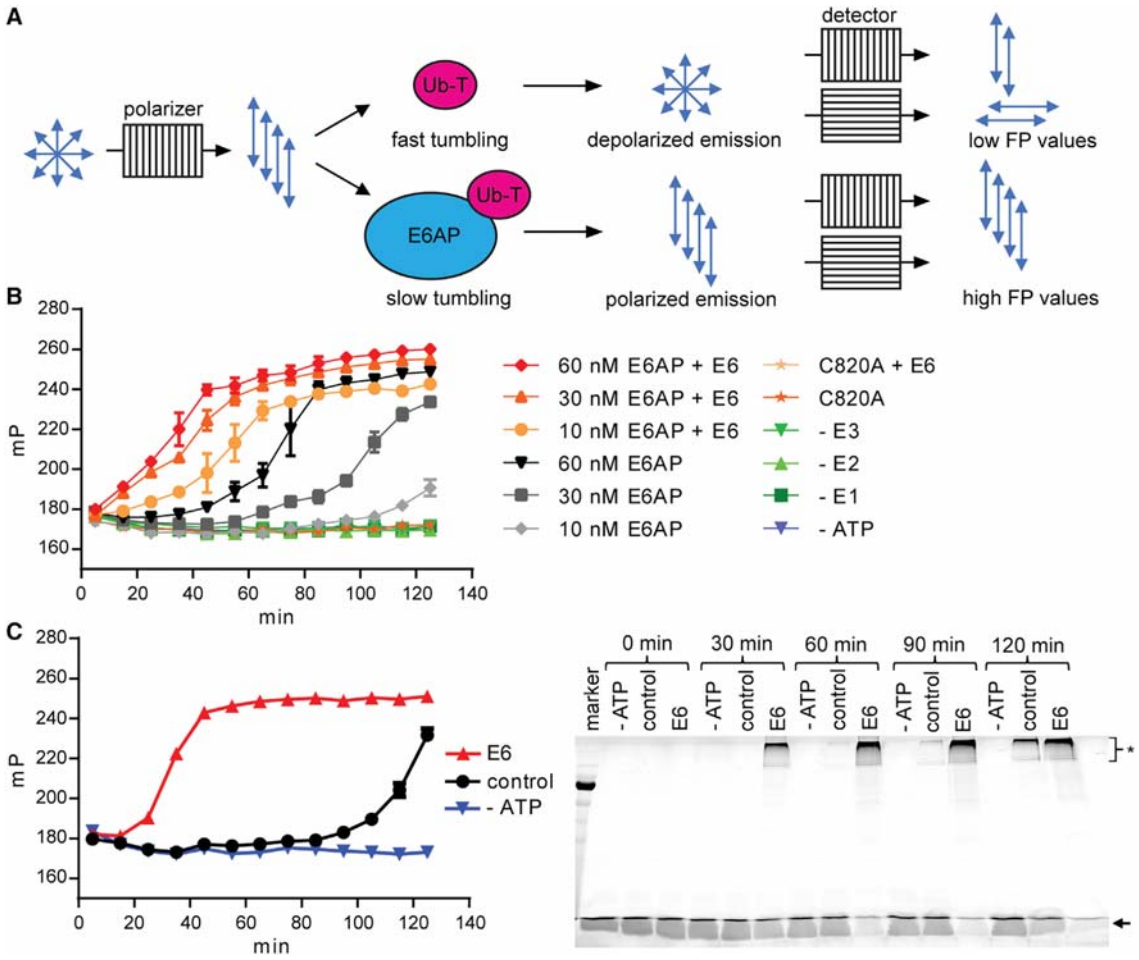

Figure 1. A Fluorescence Polarization-Based Assay to Monitor E6AP Activity

(A) Schematic of the fluorescence polarization (FP)-based ubiquitination assay. Due to Brownian motion, smaller molecules tumble faster than larger ones (i.e., free ubiquitin tumbles faster than ubiquitin attached to E6AP) and this can be monitored by FP. To do so, a fluorophore such as TAMRA is attached to ubiquitin (Ub-T). The fluorophore is excited with linearly polarized light and emits light after its fluorescence lifetime. Depending on the size of the molecule, the orientation of the fluorophore at the time of emission differs from that at the time of excitement, resulting in different FP values. The emitted light is measured by two detectors, one with a polarization filter with the same orientation as the excitation filter (F_{II}) and the other with a perpendicular-oriented filter ($F_{\perp}$). The degree of FP is calculated by the equation $FP = (F_{II} - F_{\perp})/(F_{II} + F_{\perp})$.

(B) Increasing concentrations of E6AP were incubated with E1, E2 (UbcH5b), and a mixture of Ub-T and unlabeled ubiquitin (ratio 1:10) in the absence and presence of the E6 oncoprotein. At the times indicated, FP values were determined and plotted against reaction time. Reactions in the absence of E1 or E2 or ATP were performed with 60 nM E6AP. C820A, control reaction in the presence of catalytically inactive E6AP_C820A (substitution of C820 by A; numbering according to isoform 1 of E6AP; Yamamoto et al., 1997). Error bars indicate standard deviation of three technical replicates.

(C) Left: FP-based auto-ubiquitination assay with 12 nM E6AP in the absence and presence of the E6 oncoprotein. – ATP, ubiquitination reaction in the absence of ATP. Error bars indicate standard deviation of three technical replicates. Right: At the times indicated, aliquots of the reaction mixtures were removed and analyzed by SDS-PAGE followed by fluorescence scan to visualize the migration behavior of Ub-T. The running positions of a molecular mass marker (band at 70 kDa), free TAMRA-labeled ubiquitin (arrow), and polyubiquitinated forms of E6AP (asterisk) are indicated. For further information, see Figure S1.

employed the FP-based ubiquitination assay to screen small-molecule libraries (Screening Center, University of Konstanz) for activators of E6AP. To identify potentially activating compounds, we employed rate-limiting concentrations of E6AP so that potential stimulating effects could be readily observed (Figure 1C). In contrast, supraoptimal concentrations of E1 and E2 were used to minimize the possibility that potentially activating compounds act on the level of these enzymes rather than on E6AP. Reactions in the additional presence of the E6 oncoprotein served as positive controls. As cut-off criteria, compounds were scored as positive when the reaction was stimulated by $\geq$32% at a reaction time of 45 min or $\geq$70% at 55 min, with the respective values of the control reaction in the absence of compounds and the E6-containing control reaction set to 0% and 100%, respectively.

In the initial screen with approximately 48,000 compounds at a concentration of 50 μM, 53 hits fulfilled the cutoff criteria (Figure S2; for further information on the structure of the compounds and potential common scaffolds, see Table S1). To confirm the results and to eliminate compounds that directly affect Ub-T or

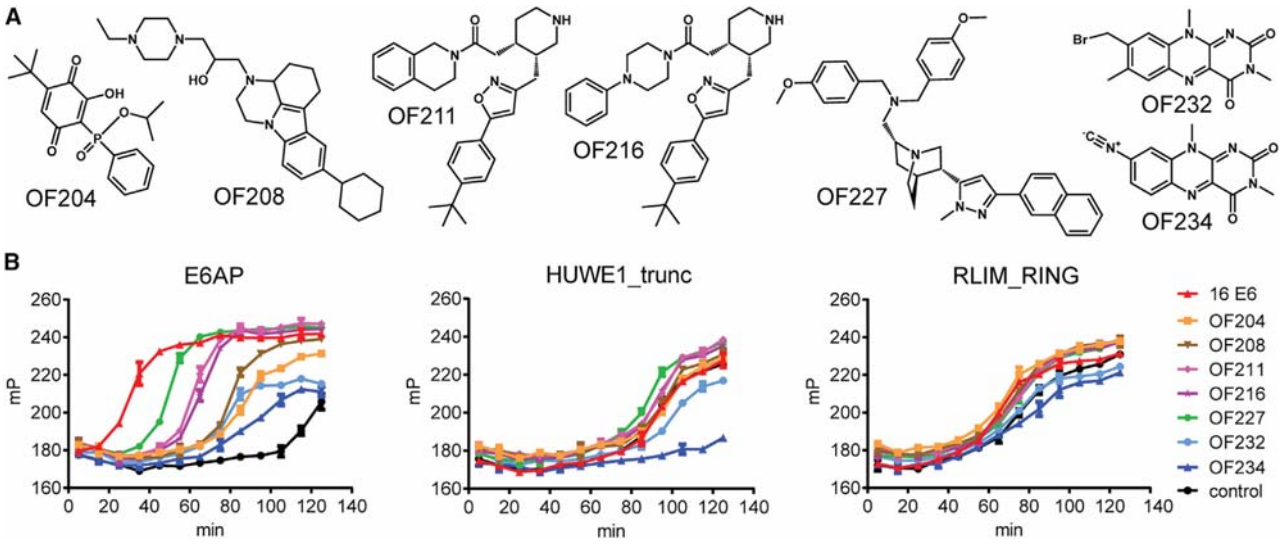

Figure 2. High-throughput Screening Identifies Small-Molecule Activators of E6AP

(A) Chemical structures of the seven compounds used in follow-up assays. Five of these (OF204, 208, 211, 216, 227) were identified in the initial screen with approximately 48,000 compounds, while two (OF232, 234) were identified in a later screen with 686 in-house synthetic compounds. The compounds were selected based on their potency and availability (OF208, 211, 216, 227, 232) and/or the presence of a common scaffold (OF211 and 216; OF204; OF232 and 234) (see also Table S1).

(B) FP-based ubiquitination assays with the seven selected compounds. The stimulating effect of the compounds (5 μM) is specific for E6AP insofar as auto-ubiquitination of an N-terminally truncated form of HUWE1 and of the RING domain of RLIM is not, or is only marginally, stimulated by these compounds. The assays were performed with 15 nM E6AP, HUWE1_trunc, and RLIM-RING. control, auto-ubiquitination was performed in the absence of any compound. Error bars indicate standard deviation of three technical replicates. For additional information, see Figure S2.

act on the level of E1 and/or E2 rather than on E6AP, we focused on those compounds that could be purchased (12) or cherry-picked (26; i.e., they were available at sufficient amounts at the Screening Center, University of Konstanz). Eighteen of these scored positive for E6AP at a concentration of 10 μM (cutoff criterion: stimulation by ≥10% at 55 min), while none scored positive with a glutathione S-transferase (GST) fusion protein of the RING domain of RLIM (RLIM_RING; Ostendorff et al., 2002) (Table S1). These results indicate the robustness of the assay and its dependence on the presence of a particular E3. Later on, 686 in-house synthetic compounds were screened at a concentration of 12.5 μM resulting in the identification of five additional, structurally related molecules with the potential to activate E6AP (Table S1). Note that the initial screens were performed with UbcH7 (Nuber et al., 1996), while secondary assays were also performed with UbcH5b, since UbcH5b supports ubiquitination by both E6AP and RLIM (Ostendorff et al., 2002; Scheffner et al., 1994) (Figures S1 and S3).

Based on potency and/or the presence of a common scaffold, we selected seven compounds for follow-up assays (structures are shown in Figure 2A; see also Table S1). As expected, their effect depends on the presence of E2 and catalytically active E6AP (Figure S3A) and is dose dependent (Figures S3B and S3C). Furthermore, their effect is specific for E6AP, as a stimulatory effect was not observed for other E3 ligases (Figure 2B). Of note, titration experiments with OF234 revealed that its stimulating effect turns into an apparent inhibitory effect at higher concentrations, not only for E6AP but also for RLIM_RING and a truncated form of HUWE1 (Figure S3D). Therefore, we studied the effect of the compounds on E1 activity in a real-time assay (Figure S3E) (Hammler et al., 2020). This showed that in particular OF232 and OF234 interfere with E1 activity in a concentration-dependent manner. Thus, OF232 and OF234, which are structurally closely related, are activators of E6AP but also inhibitors of E1. However, at low concentrations the E6AP-stimulating effect clearly supersedes the E1 inhibitory effect, justifying further characterization of their effects on E6AP activity.

Stimulating Compounds Affect the Final Transfer of Ubiquitin to Substrate Proteins

To ensure that the observed effects are not due to experimental artifacts of the TAMRA-labeled ubiquitin, we performed "standard" *in vitro* auto-ubiquitination assays in the presence of non-modified ubiquitin only. Since in these assays the reaction products are analyzed by SDS-PAGE followed by Coomassie blue staining, E6AP (as well as E1 and E2) had to be used at higher concentrations than in the FP-based assay. Thus, to detect potential stimulating effects, reactions were stopped after only 10 min (Figure 3A). Under these conditions, three of the seven compounds (OF204, OF232, OF234 at 10 μM each) showed strong stimulating effects, as evidenced by the observation that bands representing the non-modified form of E6AP and free ubiquitin were not detectable anymore with the concurrent appearance of a high-molecular-mass smear representing poly-ubiquitinated forms of E6AP.

In a simplified view, E6AP-catalyzed ubiquitination can be divided into two consecutive steps. In the first step, E6AP interacts with ubiquitin-loaded E2 (e.g., UbcH5b, UbcH7), resulting in the formation of an E6AP-ubiquitin thioester complex (Scheffner et al., 1995). In the second step, E6AP catalyzes the covalent

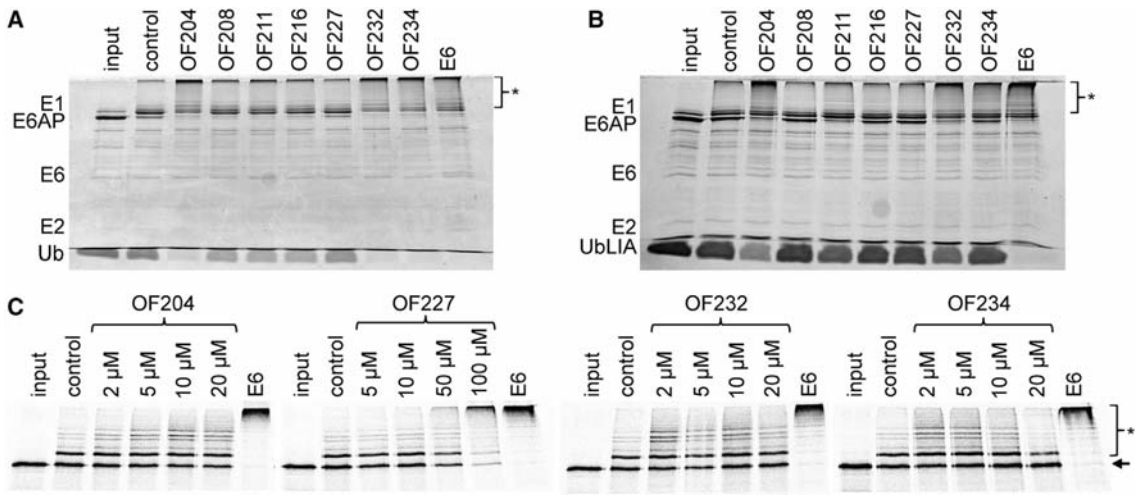

Figure 3. Validation of Small-Molecule Activators of E6AP

(A) E6AP auto-ubiquitination with wild-type ubiquitin. E6AP was incubated in the presence of E1, E2 (UbcH5b), and ubiquitin in the absence (control) or presence of the compounds indicated (10 μM) or the E6 oncoprotein under standard ubiquitination conditions (see STAR Methods). After 10 min at 30°C, reactions were stopped and the reaction mixtures subjected to SDS-PAGE followed by Coomassie blue staining. The running positions of free ubiquitin (Ub), E2, GST-16 E6, non-modified E6AP, E1, and polyubiquitinated forms of E6AP (asterisk) are indicated. Input, control reaction with DMSO was stopped at 0 min.

(B) E6AP auto-ubiquitination with UbLIA. Reactions were performed as in (A), but instead of wild-type ubiquitin, the hydrophobic patch mutant UbLIA (substitution of L8 and I44 by A) was employed and reactions were stopped after 90 min.

(C) E6AP-mediated ubiquitination of Ring1B_I53S. *In vitro*-translated radiolabeled Ring1B_I53S was incubated with E6AP, E1, E2 (UbcH5b), and UbLIA in the absence (control) or presence of increasing concentrations of the compounds indicated or GST-16 E6. After 2 h at 37°C, reactions were stopped and ubiquitination of Ring1B_I53S was analyzed by SDS-PAGE followed by fluorography. Input, control reaction with DMSO was stopped at 0 min. The migration positions of the non-modified form and the ubiquitinated forms of Ring1B_I53S are indicated by an arrow and an asterisk, respectively. Note that while all compounds act as E6AP activators, OF204 and, in particular, OF232 and 234 act also as E1 inhibitors (Figure S3E), providing an explanation for the observation that increasing concentrations of OF227 result in increased ubiquitination of Ring1B_I53S, while the E6AP stimulatory effect of OF232 and OF234 is decreasing at higher concentrations. For additional information, see Figure S3.

attachment of ubiquitin to a lysine residue of substrate proteins via isopeptide bond formation. By using a hydrophobic patch mutant of ubiquitin (UbLIA; replacement of L8 and I44 by A), we recently provided evidence that the E6 oncoprotein exerts its stimulating effect by affecting the second step (final transfer) rather than the first step (thioester complex formation) (Mortensen et al., 2015). Thus, we examined whether the compounds identified also affect the second step by performing auto-ubiquitination assays with UbLIA instead of wild-type ubiquitin (Figure 3B). Indeed, OF204 and OF232, and to a lesser extent OF234, stimulated E6AP auto-ubiquitination also when UbLIA was used as the source of ubiquitin, although not as efficiently as the E6 oncoprotein.

For four compounds (OF208, OF211, OF216, OF227), rather mild effects were observed on E6AP auto-ubiquitination under the above conditions. Therefore, these compounds were not further considered, with the exception of OF227, which showed the strongest effects of the compounds in the FP-based assay. In the following, we focused our efforts on OF204, OF227, OF232, and OF234.

To exclude the possibility that the compounds exclusively affect the ability of E6AP to ubiquitinate itself, we next performed *in vitro* ubiquitination assays with Ring1B, a known substrate of E6AP (Zaaroor-Regev et al., 2010). To this end, *in vitro*-translated radiolabeled Ring1B_I53S—an E3 ligase-deficient mutant of Ring1B (Ben-Saadon et al., 2006)—was incubated with E1, E2, and E6AP in the absence and presence of increasing concentrations of the compounds or the E6 oncoprotein. As the source of ubiquitin, UbLIA was used to facilitate the detection of potentially stimulating effects. After 90 min at 30°C, reactions were stopped and the reaction mixtures analyzed by SDS-PAGE followed by fluorography (Figure 3C). All four compounds stimulated E6AP-mediated ubiquitination in a dose-dependent manner, with OF227 showing the strongest effect. As in the FP-based assay, lower concentrations of OF232 and OF234 stimulated ubiquitination of Ring1B_I53S, while with increasing concentrations this stimulating effect decreased. Again, this observation is explained by the observation that higher concentrations of these compounds interfere with E1 activity (Figure S3E).

Rescue of the E3 Activity of AS-Derived E6AP Variants

Encouraged by the results obtained with wild-type E6AP, we set out to determine the effects of the compounds on the activity of selected E6AP variants. Approximately 10% of AS individuals harbor a maternal *UBE3A* allele with a point mutation (Sadikovic et al., 2014) frequently resulting in the expression of E6AP variants with compromised E3 activity (Cooper et al., 2004; Yi et al., 2015). As our compounds appear to affect the second step of E6AP-catalyzed ubiquitination, we were particularly interested in E6AP variants that are still capable of forming thioester complexes with ubiquitin (first step) but defective in catalyzing the subsequent covalent attachment of ubiquitin to substrate proteins (second step). Initially, we started out with six E6AP variants (C21Y, S349P, ΔS582, F583S, E584Q, Q588P; numbering

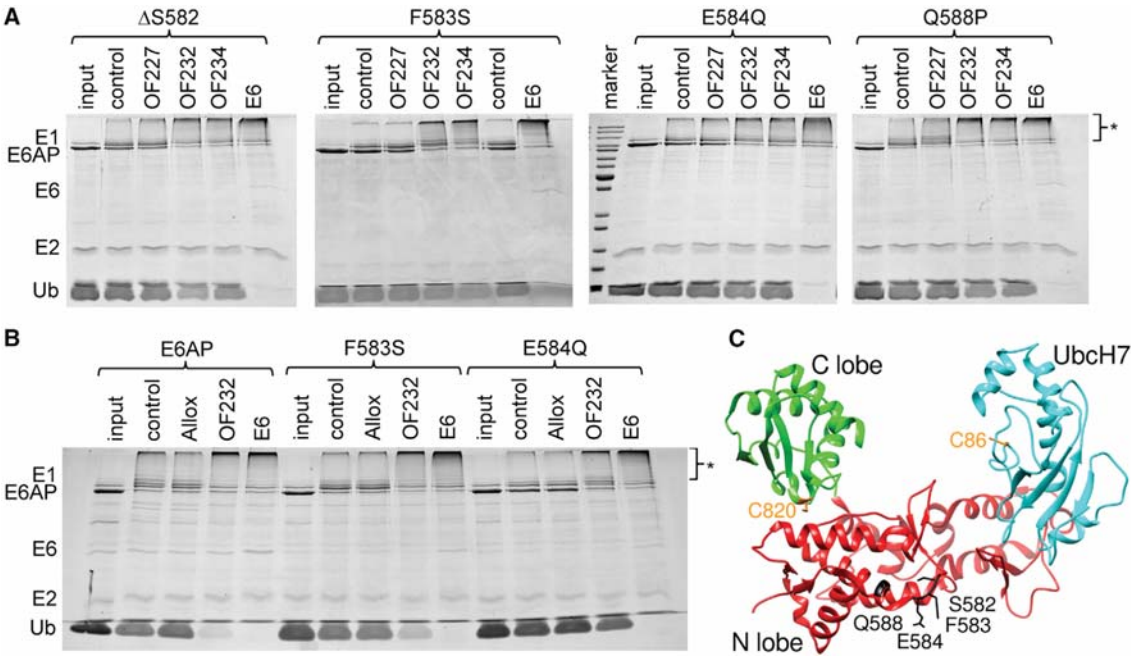

Figure 4. Small Molecules Induce Auto-ubiquitination of AS-Derived E6AP Variants

(A) The AS-derived E6AP variants ΔS582 (deletion of S582), F583S (substitution of F583 by S), E584Q (substitution of E584 by Q), and Q588P (substitution of Q588 by P) (numbering according to isoform 1 of E6AP; Yamamoto et al., 1997) were expressed in bacteria. Upon purification, similar amounts of the E6AP variants were incubated in the absence (control) and presence of the compounds indicated (10 μM) or GST-16 E6. After 90 min at 30°C, reactions were stopped and the reaction mixtures subjected to SDS-PAGE followed by Coomassie blue staining. The running positions of free ubiquitin (Ub), E2, GST-16 E6, non-modified E6AP, E1, and polyubiquitinated forms of E6AP (asterisk) are indicated. Input, control reaction with DMSO stopped at 0 min.

(B) Auto-ubiquitination reaction with E6AP and the E6AP variants F583S and E584Q in the absence (control) or presence of 10 μM alloxazine (Allox) and OF232 or GST-16 E6. Reaction time was 10 min for E6AP and 90 min for the E6AP variants. Analysis was performed as in (A).

(C) Structure of the HECT domain of E6AP in complex with UbcH7 (PDB: 1C4Z; Huang et al., 1999). The positions of the amino acid residues affected in the E6AP variants studied and the catalytic cysteine residue are indicated. The C lobe and N lobe of the HECT domain are colored in green and red, respectively. UbcH7 is colored in cyan. For additional information, see Figure S4.

according to isoform 1 of E6AP; Yamamoto et al., 1997), for which it was reported that they are proficient in forming thioester complexes with ubiquitin (Cooper et al., 2004; Yi et al., 2015) and/or for which we could show this to be the case (Figure S4A). The E3 activity of E6AP_C21Y turned out to be similar *in vitro* to the one of wild-type E6APs (Figure S4B), while E6AP_S349P showed reduced activity, but was difficult to express in, and purify from, bacteria (not shown). Thus, we did not follow up on these variants.

The E6AP variants ΔS582, F583S, E584Q, and Q588P contain point mutations that cluster in the N-terminal region of the N lobe of the HECT domain (Huang et al., 1999) (Figure 4C). Importantly, not only were these variants proficient in ubiquitin-thioester complex formation, but their deficiency in catalyzing isopeptide bond formation was efficiently rescued by the E6 oncoprotein (Figure S4C). Based on these features, we reasoned that the E3 activity of these variants may also be rescued by our compounds. Indeed, auto-ubiquitination of all four variants was restored by addition of our compounds (10 μM), with OF232 and OF234 being the most efficient (Figures 4A and S4D). Since OF232 and OF234 are alloxazine derivatives (Figure S4E), we also tested the effect of alloxazine itself. As exemplified by the experiment shown in Figure 4B (see also Figure S4E), addition of alloxazine neither rescued the E3 activity of the E6AP variants nor affected the activity of wild-type E6AP, indicating that the alloxazine scaffold of OF232 and OF234 is necessary but not sufficient for their stimulating effect. Furthermore, the compounds also strongly stimulated the ability of the E6AP variants to ubiquitinate Ring1B_I53S (Figure 5). Similar to the results obtained for wild-type E6AP, OF227 showed the strongest effect in this assay, while due to their E1 inhibitory effect, the degree of stimulation decreased with increasing concentrations of OF232 and OF234.

Since our compounds and the E6 oncoprotein were able to rescue the E3 activity of the E6AP variants *in vitro*, we wanted to know whether this can also be detected in a cellular setting. As we observed that OF227 is less cytotoxic than OF232 and OF234 (Figure S5A), we employed OF227 to study its effect on E6AP-mediated degradation of Ring1B_I53S in cotransfection experiments (Figure S5B). Indeed, addition of OF227 or coexpression of the E6 oncoprotein resulted in a reproducible increase in wild-type E6AP-mediated degradation of Ring1B_I53S. Furthermore, coexpression of the E6 oncoprotein also rescued the activity of an AS-derived E6AP variant (E584Q), while OF227 had no significant effect. These data indicate that the compounds act as potent stimulators of E6AP *in vitro* and have the potential to activate E6AP in cells. However, additional chemical modifications/derivatizations will be required to

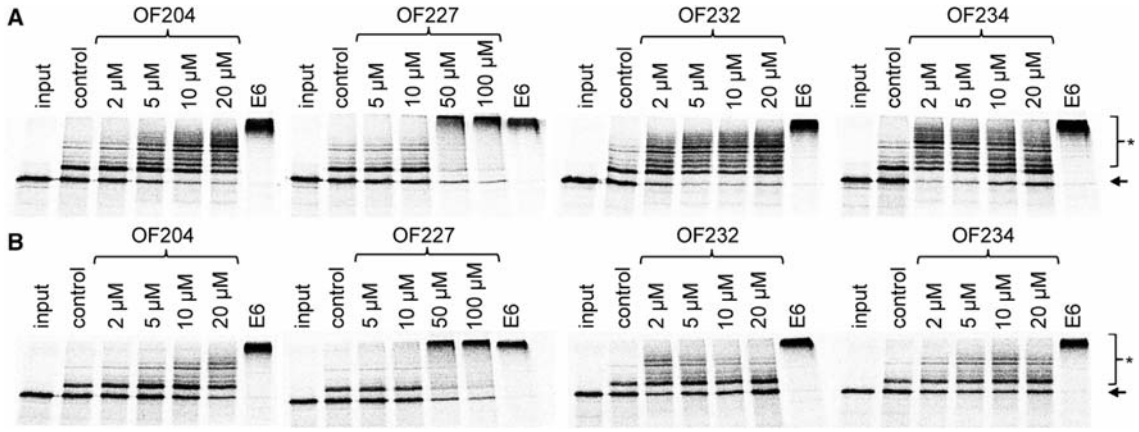

Figure 5. Small Molecules Stimulate Ubiquitination of Ring1B by AS-Derived E6AP Variants

In vitro-translated radiolabeled Ring1B_I53S was incubated with E6AP_F583S (A) and E6AP_E584Q (B), E1, and E2 (UbcH5b) in the absence (control) or presence of increasing concentrations of the compounds indicated or GST-16 E6. After 2 h at 37°C, reactions were stopped and ubiquitination of Ring1B_I53S was analyzed by SDS-PAGE followed by fluorography. Input, control reaction with DMSO was stopped at 0 min. The migration positions of the non-modified form and the ubiquitinated forms of Ring1B_I53S are indicated by an arrow and an asterisk, respectively. For additional information, see Figure S5.

increase their potency to rescue the E3 activity of AS-derived E6AP variants within cells.

OF232 Induces Structural Rearrangements in E6AP and E6AP Variants

By using quantitative (q) XL-MS, we recently showed that binding of the E6 oncoprotein induces conformational rearrangements within E6AP, thereby bringing the N- and C-terminal regions of E6AP into closer proximity or stabilizing non-covalent interactions between them (Sailer et al., 2018). Since in the *in vitro* ubiquitination assays the E6 oncoprotein and our compounds displayed similar effects on E6AP activity, we compared the effects of the compounds and the E6 oncoprotein on the structural dynamics of E6AP and AS-derived E6AP variants by qXL-MS. We put our focus on OF232, because in contrast to OF204 and OF227, we had with alloxazine an ideal control at hand.

Comparison of the overall cross-linking pattern obtained for E6AP_F583S and E6AP_E584Q with wild-type E6AP in the absence and in the presence of the E6 oncoprotein did not reveal gross differences (Figures S6B and S6C). In fact, only minor changes were observed, which fits with the observations that the two AS-derived variants are capable of forming ubiquitin-thioester complexes but are rather inactive in transferring ubiquitin to substrate proteins and that this deficiency can be rescued by the E6 oncoprotein. However, similar to the effect on wild-type E6AP (Figure 6A), binding of E6 to the E6AP variants resulted in an increased number of cross-links between the N and the C termini (Figures 6B and S6D). Most remarkably, a similar pattern was observed in the presence of OF232, while the non-activating small molecule alloxazine had a mild effect only (see Discussion). Importantly, OF204 and OF227 also elicited structural changes in E6AP_E584Q, although their exact natures might be different from those observed for OF232 (Figure S6D).

In conclusion, the results obtained by the qXL-MS approach show that both the E6 oncoprotein and OF232 induce similar patterns of up- and downregulated cross-links, and thus presumably similar structural rearrangements, in E6AP and the AS-derived E6AP variants. Since both rescue the E3 activity of the AS-derived E6AP variants, this strongly indicates that, like the E6 oncoprotein, OF232 drives E6AP into, or stabilizes, an enzymatically active conformation.

DISCUSSION

Since dysregulation of ubiquitination contributes to the development of various human disorders (Ciechanover, 2012; Popovic et al., 2014; Rape, 2018; Scheffner and Kumar, 2014), small molecules that modulate the activity of enzymes of the ubiquitin-conjugating system or the activity of deubiquitinating enzymes (DUBs) have therapeutic potential. Indeed, a number of studies indicate that not only inhibitors but also stimulators of respective enzymes represent a therapeutic option (for reviews, see Burslem and Crews, 2020; Chamberlain and Hamann, 2019; Chen et al., 2018; Clague et al., 2019; Huang and Dixit, 2016; Landre et al., 2014; Verma et al., 2020; Wertz and Wang, 2019). For example, stimulating the activity of E3 ligases and DUBs targeting proto-oncoproteins and tumor-suppressor proteins, respectively, may be beneficial in the treatment of cancers. Similarly, point mutations in the *UBE3A* gene or the *HERC2* gene affecting the E3 activity of the respective enzymes directly or indirectly by affecting their half-life and, thus, their expression levels have been causally associated with the development of AS and AS-like disorder, respectively (Harlalka et al., 2013; Yi et al., 2015). Therefore, rescuing the activity or stability of these E3 enzymes bears obvious therapeutic potential. Here, we present an easy-to-handle and robust FP-based ubiquitination assay that allows the identification of both activators and inhibitors of E3 enzymes in a high-throughput format. In addition, while this work was in its final stage, a similar FP-based assay was reported by another group (Franklin and Pruneda, 2019), indicating its general applicability for studying enzymes of the ubiquitin-conjugating machinery as well as DUBs.

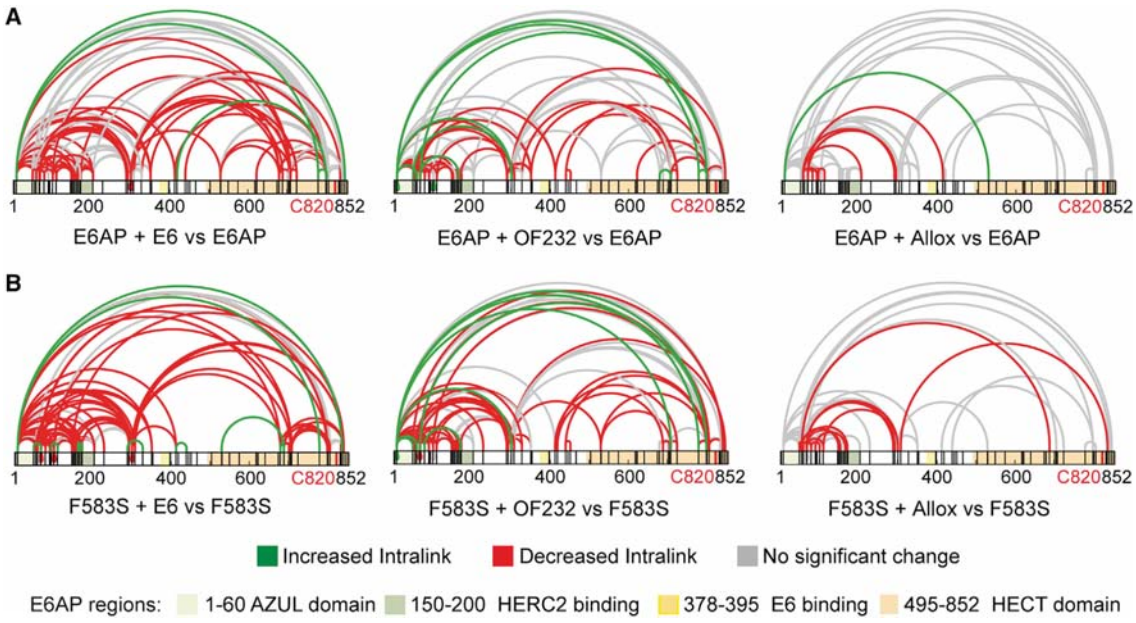

Figure 6. Small-Molecule Activator Induces Structural Rearrangements in Wild-Type E6AP and AS-Derived E6AP Variants

Patterns of intralink distribution within E6AP were determined by quantitative XL-MS as described (Sailer et al., 2018) for wild-type E6AP (A) and the AS-derived E6AP variant F583S (B) in the presence of GST-16 E6, OF232, or alloxazine (Allox) as indicated. Quantification was performed relative to E6AP alone (A) or E6AP_F583S alone (B). Cross-links that were upregulated in the presence of E6, OF232, or alloxazine are depicted in green, while downregulated links are shown in red (defined as a $\log_2$ change of greater than or equal to ±1.0). Cross-links with no significant change are depicted in gray. Lysine residues are shown in black. The catalytic cysteine residue of E6AP at position 820 is marked in red. For additional information, see Figure S6.

AS is an imprinting disorder, in which, in the majority of cases, the maternal *UBE3A* allele does not result in the expression of any protein (Buiting et al., 2016; Dagli et al., 2012). Thus, current efforts to treat AS at the molecular level aim at inducing the expression of the paternal *UBE3A* allele, e.g., by antisense approaches targeting the long non-coding RNA that interferes with expression of the paternal *UBE3A* allele (Meng et al., 2012, 2013, 2015). While such approaches hold great promise, it remains to be seen if they result in E6AP levels normally observed in the respective neuronal cells. Thus, we propose that compounds stimulating the activity of wild-type E6AP may prove beneficial in combinatorial treatment regimens. Furthermore, approximately 10% of AS individuals harbor a maternal *UBE3A* allele with a point mutation resulting in the expression of E6AP variants with compromised E3 activity. It was previously shown that the E3 activity of AS-derived E6AP variants can be affected at different levels (Avagliano Trezza et al., 2019; Cooper et al., 2004; Yi et al., 2015). Some display a shortened half-life, e.g., due to folding problems or increased auto-ubiquitination activity, resulting in levels insufficient for E6AP to exert its normal physiological functions, while others have an altered subcellular localization, thereby promoting AS development. A third class of E6AP variants harbor mutations in the catalytic HECT domain directly affecting the E3 activity. Such mutations can affect the ability of E6AP to interact with its cognate E2 enzymes (UbcH7, UbcH5), to form thioester complexes with ubiquitin, or to catalyze the final attachment of ubiquitin to substrate proteins. The property of the compounds identified here to stimulate and/or rescue E3 activity is likely to be limited to E6AP variants with residual E3 activity, with residual being defined as having at least the ability to form thioester complexes with ubiquitin. Yet, our FP-based assay is in general suited to identifying stimulating/rescuing compounds for any E6AP variant with a single amino acid substitution, except for those displaying altered protein-protein interaction properties (Avagliano Trezza et al., 2019; Kühnle et al., 2018) resulting, for instance, in aberrant subcellular localization.

Here, we focused our efforts on E6AP variants that are proficient for ubiquitin thioester complex formation and whose activity can be rescued by the E6 oncoprotein. By using qXL-MS (Sailer et al., 2018), we recently provided evidence that the E6 oncoprotein affects the conformational dynamics of E6AP, and thereby E6AP activity, by stabilizing an E6AP conformation or conformational ensemble enabling the final transfer of ubiquitin from E6AP to lysine residues of substrate proteins or ubiquitin itself, resulting in ubiquitin chain formation. Remarkably, in-depth qXL-MS analysis of the effect of one of the stimulating compounds (OF232) revealed that its effect on the conformational dynamics of E6AP is similar to that of the E6 oncoprotein. Thus, from a functional aspect, OF232—and possibly also OF204 and OF227, the structural effects of which were studied in less detail, as only limited amounts were available to us—can be considered as an E6 analog. Although we do not know the exact binding site of OF232 on E6AP, this, the observation that OF232 has no detectable effect on the isolated HECT domain of E6AP (data not shown), and the results obtained with alloxazine suggest that, like the E6 oncoprotein, OF232 has its primary binding site within the N-terminal region of E6AP. Alloxazine, the basic scaffold of OF232, does not stimulate E6AP activity and in comparison to OF232 has a small but

reproducible effect on E6AP conformation. Again, this effect is mainly observed within the N-terminal region of E6AP, suggesting that it contains the primary binding site for alloxazine and OF232 and that additional properties of OF232 are required to exert its stimulating/rescuing effect. It should be noted that we have no evidence that OF232 or any of the other compounds become covalently attached to E6AP, indicating that their stimulating/rescuing effects are mediated by non-covalent interactions. Confirmation of the hypothesis that OF232 stabilizes an enzymatically more active conformation of E6AP by binding within the N-terminal region of E6AP will have to await solution of the structure of E6AP in the absence and presence of OF232. Nonetheless, the data presented here suggest that qXL-MS represents an attractive tool to study the interactions of proteins with small molecules, in particular when the structure of the protein of interest is not available. In this context, the availability of small molecules such as OF232 that stabilize a distinct conformation or conformational ensemble may prove helpful in obtaining a crystal structure of full-length E6AP.

The effects of the small-molecule activators of E6AP studied in more detail (OF204, OF227, OF232, OF234) are specific with respect to the E3 ligases tested. Nonetheless, like for other small-molecule-protein interactions, it can be expected that they also target other proteins or biomolecules. In fact, OF204, OF232, and OF234 interfere with E1 activity, although at concentrations exceeding those required for E6AP stimulation (Figure S3D). Thus, in future studies the compounds need to be derivatized such that their stimulating potency is increased and their cytotoxicity is simultaneously decreased. The potential efficacy of such compounds can then be tested in AS mouse models or using human induced pluripotent stem cell-based systems expressing respective AS-derived E6AP variants (Fink et al., 2017; Sonzogni et al., 2018). In conclusion, we propose that the small molecules identified here as E6AP activators have the potential to serve as lead structures for the development of drugs for the treatment of AS.

SIGNIFICANCE

E3 ubiquitin ligases determine which proteins are posttranslationally modified with ubiquitin, thereby regulating many cellular processes. The ubiquitin ligase E6AP has been causally associated with three distinct clinical pictures, cervical cancer and the neurodevelopmental disorders Angelman syndrome (AS) and Dup15q syndrome. Thus, E6AP represents an impressive example of the notion that dysregulation of ubiquitination plays an important role in the development of human disease. Genetic aberrations of the *UBE3A* gene, which encodes E6AP, underlie the development of AS. Approximately 10% of AS individuals harbor *UBE3A* genes with point mutations, frequently resulting in the expression of full-length E6AP variants with defective E3 activity. We, therefore, hypothesized that it should be possible to rescue the activity of such variants using small molecules. To address this possibility, we developed a high-throughput screening assay based on fluorescence polarization to monitor the activity of ubiquitin ligases in general and E6AP in particular. We identified several compounds that not only stimulate the activity of wild-type E6AP, but also rescue the activity of distinct AS-derived E6AP variants. Thus, we propose that these compounds represent potential lead structures for the design of drugs for AS treatment.

STAR★METHODS

Detailed methods are provided in the online version of this paper and include the following:

- KEY RESOURCES TABLE
- RESOURCE AVAILABILITY
  - Lead Contact
  - Materials Availability
  - Data and Code Availability
- EXPERIMENTAL MODEL AND SUBJECT DETAILS
- METHOD DETAILS
  - Site-Directed Mutagenesis
  - Expression and Purification of His-E6AP
  - Expression and Purification of E6AP_HECT
  - Expression and Purification of GST Fusion Proteins
  - Expression and Purification of E1
  - Expression and Purification of E2 Enzymes
  - Expression and Purification of UbLIA
  - TAMRA-Labeling of Ubiquitin
  - Analysis of TAMRA-Labeled Ubiquitin (Ub-T)
  - FP-Based *In Vitro* Ubiquitination Assay
  - High-throughput Screening
  - EC50 Determination
  - *In Vitro* Auto-ubiquitination Assay
  - *In Vitro* Ubiquitination of Ring1B_I53S
  - Ubiquitin Thioester Complex Formation Assay
  - Degradation of Ectopically Expressed Ring1B_I53S
  - Cytotoxicity Assay
  - qXL-MS Analysis
- QUANTIFICATION AND STATISTICAL ANALYSIS

ACKNOWLEDGMENTS

We are grateful to Silke Büstorf and Nicole Richter-Müller for technical support, Silke Müller and the Screening Center of the University of Konstanz for support with high-throughput screening, and Andreas Marquardt and Anna Sladewska-Marquardt of the Proteomics Center of the University of Konstanz for support with mass spectrometric experiments. F.S. acknowledges funding by the Emmy Noether Program of the Deutsche Forschungsgemeinschaft (STE 2517/1-1). This work was supported by the Deutsche Forschungsgemeinschaft (German Research Foundation), 406631249.

AUTHOR CONTRIBUTIONS

Conceptualization, F.O., F.M., F.S., and M.S.; Methodology, F.O., F.M., D.H., K.H.G., A.M., F.S., and M.S.; Investigation, F.O., F.M., J.J., and D.H.; Writing – Original Draft, F.O. and M.S.; Writing – Reviewing & Editing, F.O., F.M., J.J., D.H., K.H.G., A.M., C.L.S., S.J.C., F.S., and M.S.; Funding Acquisition, F.S. and M.S.; Resources, C.L.S. and S.J.C.; Supervision, A.M., S.J.C., F.S., and M.S.

DECLARATION OF INTERESTS

The authors declare no competing interests.

REFERENCES

Adhikary, S., Marinoni, F., Hock, A., Hulleman, E., Popov, N., Beier, R., Bernard, S., Quarto, M., Capra, M., Goettig, S., et al. (2005). The ubiquitin ligase HectH9 regulates transcriptional activation by Myc and is essential for tumor cell proliferation. Cell *123*, 409–421.

Avagliano Trezza, R., Sonzogni, M., Bossuyt, S.N.V., Zampeta, F.I., Punt, A.M., van den Berg, M., Rotaru, D.C., Koene, L.M.C., Munshi, S.T., Stedehouder, J., et al. (2019). Loss of nuclear UBE3A causes electrophysiological and behavioral deficits in mice and is associated with Angelman syndrome. Nat. Neurosci. *22*, 1235–1247.

Ben-Saadon, R., Zaaroor, D., Ziv, T., and Ciechanover, A. (2006). The polycomb protein Ring1B generates self atypical mixed ubiquitin chains required for its in vitro histone H2A ligase activity. Mol. Cell *24*, 701–711.

Berthold, M.R., Cebron, N., Dill, F., Gabriel, T.R., Kotter, T., Meinl, T., Ohl, P., Sieb, C., Thiel, K., and Wiswedel, B. (2008). KNIME: the Konstanz information miner. In Data Analysis, Machine Learning and Applications. Studies in Classification, Data Analysis, and Knowledge Organization, C. Preisach, H. Burkhardt, L. Schmidt-Thieme, and R. Decker, eds. (Springer).

Buiting, K., Williams, C., and Horsthemke, B. (2016). Angelman syndrome - insights into a rare neurogenetic disorder. Nat. Rev. Neurol. *12*, 584–593.

Burslem, G.M., and Crews, C.M. (2020). Proteolysis-targeting chimeras as therapeutics and tools for biological discovery. Cell *181*, 102–114.

Chamberlain, P.P., and Hamann, L.G. (2019). Development of targeted protein degradation therapeutics. Nat. Chem. Biol. *15*, 937–944.

Chen, D., Gehringer, M., and Lorenz, S. (2018). Developing small-molecule inhibitors of HECT-type ubiquitin ligases for therapeutic applications: challenges and opportunities. Chembiochem *19*, 2123–2135.

Ciechanover, A. (2012). Intracellular protein degradation: from a vague idea thru the lysosome and the ubiquitin-proteasome system and onto human diseases and drug targeting. Biochim. Biophys. Acta *1824*, 3–13.

Clague, M.J., Urbe, S., and Komander, D. (2019). Breaking the chains: deubiquitylating enzyme specificity begets function. Nat. Rev. Mol. Cell Biol. *20*, 338–352.

Cooper, E.M., Hudson, A.W., Amos, J., Wagstaff, J., and Howley, P.M. (2004). Biochemical analysis of Angelman syndrome-associated mutations in the E3 ubiquitin ligase E6-associated protein. J. Biol. Chem. *279*, 41208–41217.

Dagli, A., Buiting, K., and Williams, C.A. (2012). Molecular and clinical aspects of Angelman syndrome. Mol. Syndromol. *2*, 100–112.

Fink, J.J., Robinson, T.M., Germain, N.D., Sirois, C.L., Bolduc, K.A., Ward, A.J., Rigo, F., Chamberlain, S.J., and Levine, E.S. (2017). Disrupted neuronal maturation in Angelman syndrome-derived induced pluripotent stem cells. Nat. Commun. *8*, 15038.

Franklin, T.G., and Pruneda, J.N. (2019). A high-throughput assay for monitoring ubiquitination in real time. Front. Chem. *7*, 816.

Glessner, J.T., Wang, K., Cai, G., Korvatska, O., Kim, C.E., Wood, S., Zhang, H., Estes, A., Brune, C.W., Bradfield, J.P., et al. (2009). Autism genome-wide copy number variation reveals ubiquitin and neuronal genes. Nature *459*, 569–573.

Hall, M.D., Yasgar, A., Peryea, T., Braisted, J.C., Jadhav, A., Simeonov, A., and Coussens, N.P. (2016). Fluorescence polarization assays in high-throughput screening and drug discovery: a review. Methods Appl. Fluores. *4*, 022001.

Hammler, D., Stuber, K., Offensperger, F., Scheffner, M., Zumbusch, A., and Marx, A. (2020). Fluorescently labelled ATP analogues for direct monitoring of ubiquitin activation. Chemistry *26*, 6279–6284.

Harlalka, G.V., Baple, E.L., Cross, H., Kuhnle, S., Cubillos-Rojas, M., Matentzoglu, K., Patton, M.A., Wagner, K., Coblentz, R., Ford, D.L., et al. (2013). Mutation of HERC2 causes developmental delay with Angelman-like features. J. Med. Genet. *50*, 65–73.

Hogart, A., Wu, D., LaSalle, J.M., and Schanen, N.C. (2010). The comorbidity of autism with the genomic disorders of chromosome 15q11.2-q13. Neurobiol. Dis. *38*, 181–191.

Honda, R., Tanaka, H., and Yasuda, H. (1997). Oncoprotein MDM2 is a ubiquitin ligase E3 for tumor suppressor p53. FEBS Lett. *420*, 25–27.

Hsiao, J.S., Germain, N.D., Wilderman, A., Stoddard, C., Wojenski, L.A., Villafano, G.J., Core, L., Cotney, J., and Chamberlain, S.J. (2019). A bipartite boundary element restricts UBE3A imprinting to mature neurons. Proc. Natl. Acad. Sci. U S A *116*, 2181–2186.

Huang, L., Kinnucan, E., Wang, G., Beaudenon, S., Howley, P.M., Huibregtse, J.M., and Pavletich, N.P. (1999). Structure of an E6AP-UbcH7 complex: insights into ubiquitination by the E2-E3 enzyme cascade. Science *286*, 1321–1326.

Huang, X., and Aulabaugh, A. (2016). Application of fluorescence polarization in HTS assays. Methods Mol. Biol. *1439*, 115–130.

Huang, X., and Dixit, V.M. (2016). Drugging the undruggables: exploring the ubiquitin system for drug development. Cell Res. *26*, 484–498.

Huibregtse, J.M., Scheffner, M., Beaudenon, S., and Howley, P.M. (1995). A family of proteins structurally and functionally related to the E6-AP ubiquitin-protein ligase. Proc. Natl. Acad. Sci. U S A *92*, 2563–2567.

Huibregtse, J.M., Scheffner, M., and Howley, P.M. (1993). Cloning and expression of the cDNA for E6-AP, a protein that mediates the interaction of the human papillomavirus E6 oncoprotein with p53. Mol. Cell. Biol. *13*, 775–784.

Huibregtse, J.M., Scheffner, M., and Howley, P.M. (1991). A cellular protein mediates association of p53 with the E6 oncoprotein of human papillomavirus types 16 or 18. EMBO J. *10*, 4129–4135.

Khatri, N., and Man, H.Y. (2019). The autism and Angelman syndrome protein Ube3A/E6AP: the gene, E3 ligase ubiquitination targets and neurobiological functions. Front. Mol. Neurosci. *12*, 109.

Kim, H.C., and Huibregtse, J.M. (2009). Polyubiquitination by HECT E3s and the determinants of chain type specificity. Mol. Cell. Biol. *29*, 3307–3318.

Kishino, T., Lalande, M., and Wagstaff, J. (1997). UBE3A/E6-AP mutations cause Angelman syndrome. Nat. Genet. *15*, 70–73.

Kuballa, P., Matentzoglu, K., and Scheffner, M. (2007). The role of the ubiquitin ligase E6-AP in human papillomavirus E6-mediated degradation of PDZ domain-containing proteins. J. Biol. Chem. *282*, 65–71.

Kühnle, S., Kogel, U., Glockzin, S., Marquardt, A., Ciechanover, A., Matentzoglu, K., and Scheffner, M. (2011). Physical and functional interaction of the HECT ubiquitin-protein ligases E6AP and HERC2. J. Biol. Chem. *286*, 19410–19416.

Kühnle, S., Martinez-Noel, G., Leclere, F., Hayes, S.D., Harper, J.W., and Howley, P.M. (2018). Angelman syndrome-associated point mutations in the Zn(2+)-binding N-terminal (AZUL) domain of UBE3A ubiquitin ligase inhibit binding to the proteasome. J. Biol. Chem. *293*, 18387–18399.

Kumar, S., Talis, A.L., and Howley, P.M. (1999). Identification of HHR23A as a substrate for E6-associated protein-mediated ubiquitination. J. Biol. Chem. *274*, 18785–18792.

Landre, V., Rotblat, B., Melino, S., Bernassola, F., and Melino, G. (2014). Screening for E3-Ubiquitin ligase inhibitors: challenges and opportunities. Oncotarget *5*, 7988–8013.

LaSalle, J.M., Reiter, L.T., and Chamberlain, S.J. (2015). Epigenetic regulation of UBE3A and roles in human neurodevelopmental disorders. Epigenomics *7*, 1213–1228.

Leitner, A., Walzthoeni, T., and Aebersold, R. (2014). Lysine-specific chemical cross-linking of protein complexes and identification of cross-linking sites using LC-MS/MS and the xQuest/xProphet software pipeline. Nat. Protoc. *9*, 120–137.

Lemak, A., Yee, A., Bezsonova, I., Dhe-Paganon, S., and Arrowsmith, C.H. (2011). Zn-binding AZUL domain of human ubiquitin protein ligase Ube3A. J. Biomol. NMR *51*, 185–190.

Margolis, S.S., Salogiannis, J., Lipton, D.M., Mandel-Brehm, C., Wills, Z.P., Mardinly, A.R., Hu, L.D., Greer, P.L., Bikoff, J.B., Ho, H.Y.H., et al. (2010). EphB-mediated degradation of the RhoA GEF Ephexin5 relieves a developmental brake on excitatory synapse formation. Cell *143*, 442–455.

Martinez-Zapien, D., Ruiz, F.X., Poirson, J., Mitschler, A., Ramirez, J., Forster, A., Cousido-Siah, A., Masson, M., Vande Pol, S., Podjarny, A., et al. (2016). Structure of the E6/E6AP/p53 complex required for HPV-mediated degradation of p53. Nature *529*, 541–545.

Matsuura, T., Sutcliffe, J.S., Fang, P., Galjaard, R.J., Jiang, Y.H., Benton, C.S., Rommens, J.M., and Beaudet, A.L. (1997). De novo truncating mutations in E6-AP ubiquitin-protein ligase gene (UBE3A) in Angelman syndrome. Nat. Genet. *15*, 74–77.

Meng, L.Y., Person, R.E., and Beaudet, A.L. (2012). Ube3a-ATS is an atypical RNA polymerase II transcript that represses the paternal expression of Ube3a. Hum. Mol. Genet. *21*, 3001–3012.

Meng, L., Person, R.E., Huang, W., Zhu, P.J., Costa-Mattioli, M., and Beaudet, A.L. (2013). Truncation of Ube3a-ATS unsilences paternal Ube3a and ameliorates behavioral defects in the Angelman syndrome mouse model. PLoS Genet. *9*, e1004039.

Meng, L.Y., Ward, A.J., Chun, S., Bennett, C.F., Beaudet, A.L., and Rigo, F. (2015). Towards a therapy for Angelman syndrome by targeting a long noncoding RNA. Nature *518*, 409–412.

Mortensen, F., Schneider, D., Barbic, T., Sladewska-Marquardt, A., Kühnle, S., Marx, A., and Scheffner, M. (2015). Role of ubiquitin and the HPV E6 oncoprotein in E6AP-mediated ubiquitination. Proc. Natl. Acad. Sci. U S A *112*, 9872–9877.

Mulherkar, S.A., Sharma, J., and Jana, N.R. (2009). The ubiquitin ligase E6-AP promotes degradation of alpha-synuclein. J. Neurochem. *110*, 1955–1964.

Nuber, U., Schwarz, S., Kaiser, P., Schneider, R., and Scheffner, M. (1996). Cloning of human ubiquitin-conjugating enzymes UbcH6 and UbcH7 (E2-F1) and characterization of their interaction with E6-AP and RSP5. J. Biol. Chem. *271*, 2795–2800.

Nuber, U., Schwarz, S.E., and Scheffner, M. (1998). The ubiquitin-protein ligase E6-associated protein (E6-AP) serves as its own substrate. Eur. J. Biochem. *254*, 643–649.

Ostendorff, H.P., Peirano, R.I., Peters, M.A., Schluter, A., Bossenz, M., Scheffner, M., and Bach, I. (2002). Ubiquitination-dependent cofactor exchange on LIM homeodomain transcription factors. Nature *416*, 99–103.

Perez-Riverol, Y., Csordas, A., Bai, J., Bernal-Llinares, M., Hewapathirana, S., Kundu, D.J., Inuganti, A., Griss, J., Mayer, G., Eisenacher, M., et al. (2019). The PRIDE database and related tools and resources in 2019: improving support for quantification data. Nucleic Acids Res. *47*, D442–D450.

Popovic, D., Vucic, D., and Dikic, I. (2014). Ubiquitination in disease pathogenesis and treatment. Nat. Med. *20*, 1242–1253.

Rape, M. (2018). Ubiquitylation at the crossroads of development and disease. Nat. Rev. Mol. Cell Biol. *19*, 59–70.

Rougeulle, C., Glatt, H., and Lalande, M. (1997). The Angelman syndrome candidate gene, UBE3A/E6-AP, is imprinted in brain. Nat. Genet. *17*, 14–15.

Runte, M., Huttenhofer, A., Gross, S., Kiefmann, M., Horsthemke, B., and Buiting, K. (2001). The IC-SNURF-SNRPN transcript serves as a host for multiple small nucleolar RNA species and as an antisense RNA for UBE3A. Hum. Mol. Genet. *10*, 2687–2700.

Sadikovic, B., Fernandes, P., Zhang, V.W., Ward, P.A., Miloslavskaya, I., Rhead, W., Rosenbaum, R., Gin, R., Roa, B., and Fang, P. (2014). Mutation update for UBE3A variants in Angelman syndrome. Hum. Mutat. *35*, 1407–1417.

Sailer, C., Offensperger, F., Julier, A., Kammer, K.M., Walker-Gray, R., Gold, M.G., Scheffner, M., and Stengel, F. (2018). Structural dynamics of the E6AP/UBE3A-E6-p53 enzyme-substrate complex. Nat. Commun. *9*, 4441.

Scheffner, M., Huibregtse, J.M., and Howley, P.M. (1994). Identification of a human ubiquitin-conjugating enzyme that mediates the E6-AP-dependent ubiquitination of p53. Proc. Natl. Acad. Sci. U S A *91*, 8797–8801.

Scheffner, M., Huibregtse, J.M., Vierstra, R.D., and Howley, P.M. (1993). The HPV-16 E6 and E6-AP complex functions as a ubiquitin-protein ligase in the ubiquitination of p53. Cell *75*, 495–505.

Scheffner, M., and Kumar, S. (2014). Mammalian HECT ubiquitin-protein ligases: biological and pathophysiological aspects. Biochim. Biophys. Acta *1843*, 61–74.

Scheffner, M., Nuber, U., and Huibregtse, J.M. (1995). Protein ubiquitination involving an E1-E2-E3 enzyme ubiquitin thioester cascade. Nature *373*, 81–83.

Shang, F., Deng, G., Liu, Q., Guo, W., Haas, A.L., Crosas, B., Finley, D., and Taylor, A. (2005). Lys6-modified ubiquitin inhibits ubiquitin-dependent protein degradation. J. Biol. Chem. *280*, 20365–20374.

Sonzogni, M., Wallaard, I., Santos, S.S., Kingma, J., du Mee, D., van Woerden, G.M., and Elgersma, Y. (2018). A behavioral test battery for mouse models of Angelman syndrome: a powerful tool for testing drugs and novel Ube3a mutants. Mol. Autism *9*, 47.

Sun, A.X., Yuan, Q., Fukuda, M., Yu, W., Yan, H., Lim, G.G.Y., Nai, M.H., D'Agostino, G.A., Tran, H.D., Itahana, Y., et al. (2019). Potassium channel dysfunction in human neuronal models of Angelman syndrome. Science *366*, 1486–1492.

Sutcliffe, J.S., Jiang, Y.H., Galijaard, R.J., Matsuura, T., Fang, P., Kubota, T., Christian, S.L., Bressler, J., Cattanach, B., Ledbetter, D.H., et al. (1997). The E6-AP ubiquitin-protein ligase (UBE3A) gene is localized within a narrowed Angelman syndrome critical region. Genome Res. *7*, 368–377.

Verma, R., Mohl, D., and Deshaies, R.J. (2020). Harnessing the power of proteolysis for targeted protein inactivation. Mol. Cell *77*, 446–460.

Wallace, N.A., and Galloway, D.A. (2015). Novel functions of the human papillomavirus E6 oncoproteins. Annu. Rev. Virol. *2*, 403–423.

Walzthoeni, T., Joachimiak, L.A., Rosenberger, G., Rost, H.L., Malmstrom, L., Leitner, A., Frydman, J., and Aebersold, R. (2015). xTract: software for characterizing conformational changes of protein complexes by quantitative cross-linking mass spectrometry. Nat. Methods *12*, 1185–1190.

Wang, M., and Pickart, C.M. (2005). Different HECT domain ubiquitin ligases employ distinct mechanisms of polyubiquitin chain synthesis. EMBO J. *24*, 4324–4333.

Wertz, I.E., and Wang, X. (2019). From discovery to bedside: targeting the ubiquitin system. Cell Chem. Biol. *26*, 156–177.

White, E.A., and Howley, P.M. (2013). Proteomic approaches to the study of papillomavirus-host interactions. Virology *435*, 57–69.

Yamamoto, Y., Huibregtse, J.M., and Howley, P.M. (1997). The human E6-AP gene (UBE3A) encodes three potential protein isoforms generated by differential splicing. Genomics *41*, 263–266.

Yi, J.J., Berrios, J., Newbern, J.M., Snider, W.D., Philpot, B.D., Hahn, K.M., and Zylka, M.J. (2015). An autism-linked mutation disables phosphorylation control of UBE3A. Cell *162*, 795–807.

Zaaroor-Regev, D., de Bie, P., Scheffner, M., Noy, T., Shemer, R., Heled, M., Stein, I., Pikarsky, E., and Ciechanover, A. (2010). Regulation of the polycomb protein Ring1B by self-ubiquitination or by E6-AP may have implications to the pathogenesis of Angelman syndrome. Proc. Natl. Acad. Sci. U S A *107*, 6788–6793.

Zhang, J.H., Chung, T.D.Y., and Oldenburg, K.R. (1999). A simple statistical parameter for use in evaluation and validation of high throughput screening assays. J. Biomol. Screen. *4*, 67–73.

Zheng, N., and Shabek, N. (2017). Ubiquitin ligases: structure, function, and regulation. Annu. Rev. Biochem. *86*, 129–157.

STAR★METHODS

KEY RESOURCES TABLE

REAGENT or RESOURCE	SOURCE	IDENTIFIER
Antibodies		
Anti-HA.11 monoclonal antibody (clone 16B12)	BioLegend	Cat#901516; RRID: AB_282020
Bacterial and Virus Strains		
E. coli Rosetta 2 (DE3)	Novagen	Cat#71397
E. coli BL21 (DE3)	Novagen	Cat#69450
E. coli pLysS	Novagen	Cat#69451
E. coli XL-10 gold	Stratagene	Cat#200314
Baculovirus encoding human E1	W. Krek, ETH Zurich	N/A
Chemicals, Peptides, and Recombinant Proteins		
Ubiquitin from bovine erythrocytes	Sigma-Aldrich	Cat#U6352
5-(and-6)-Carboxytetramethylrhodamine-Succinimidyl Ester (5(6)-TAMRA, SE), mixed isomers	Invitrogen	Cat#C1171
Ubiquitin-TAMRA (Ub-T)	This study	N/A
DpnI	NEB	Cat#R0176
PFU Turbo polymerase	Agilent	Cat#600250
E/Z view anti-HA agarose beads	Sigma-Aldrich	Cat#E6779
Aprotinin	Carl Roth	Cat#A162
Leupeptin	Carl Roth	Cat#CN33
Pefabloc SC	Carl Roth	Cat#154
OF204	Vitas-M laboratory	Cat#STK682896
OF208	ChemDiv	Cat#STK722575
OF211	AnalytiCon Discovery	Cat#NAT14-350422
OF216	AnalytiCon Discovery	Cat#NAT14-350412
OF227	AnalytiCon Discovery	Cat#NAT13-262412
OF232	Screening Center Uni Konstanz	N/A
OF234	Screening Center Uni Konstanz	N/A
Alloxazine	Sigma-Aldrich	Cat#A28651
DSS-H12/D12 (Disuccinimidyl suberate)	Creative Molecules	Cat#001S
Trypsin	Promega	Cat#V511C
Critical Commercial Assays		
TNT T7-coupled reticulocyte lysate system	Promega	Cat#L4610
Deposited Data		
Mass spectrometry proteomics data (raw files, xQuest and xTract search output files)	This paper	PRIDE: PXDPXD020602
Experimental Models: Cell Lines		
H1299 (*Homo sapiens*: non-small cell lung carcinoma)	ATCC	Cat#CRL-5803
H1299 K3 (H1299 cells selected for stable RNAi-mediated knockdown of E6AP expression)	(Kuballa et al., 2007)	N/A
Recombinant DNA		
pET21a-UbcH5b-opt/pET21a-UbcH7-opt	(Mortensen et al., 2015)	N/A
pTZ_E12-E6AP-opt	Trenzyme GmbH (Konstanz, Germany)	N/A
pGEX-16 E6	(Huibregtse et al., 1991)	N/A
pTZ_E12-E6AP-opt_ΔS582	this study	N/A
pTZ_E12-E6AP-opt_F583S	this study	N/A

(*Continued on next page*)

Continued

REAGENT or RESOURCE	SOURCE	IDENTIFIER
pTZ_E12-E6AP-opt_E584Q	this study	N/A
pTZ_E12-E6AP-opt_Q588P	this study	N/A
pcDNA3_HA-E6AP	(Kühnle et al., 2011)	N/A
pcDNA3_HA-E6AP_E584Q	this study	N/A
pcDNA3_HA-16 E6	(Kuballa et al., 2007)	N/A
pcDNA3_HA-Ring1B_I53S	(Zaaroor-Regev et al., 2010)	N/A
Software and Algorithms		
KNIME 4.1.0	KNIME AG	https://www.knime.com/
Prism 6	GraphPad	https://www.graphpad.com/scientific-software/prism/
AIDA Image Analysis software	Elysia-Raytest	https://www.elysia-raytest.com/de/cataloglight/c30~aida-image-analysis-software
UCSF Chimera	RVBI	https://www.cgl.ucsf.edu/chimera/
xQuest/xProphet 2.1.3	T. Walzthoeni, ETH Zuerich	http://proteomics.ethz.ch/cgi-bin/xquest2_cgi/index.cgi
xTract 1.0.2	T. Walzthoeni, ETH Zuerich	http://proteomics.ethz.ch/cgi-bin/xtract_cgi/index.cgi
xiNET	Rappsilber Lab	http://crosslinkviewer.org/
Xcalibur 3.0.63	ThermoFisher Scientific	https://www.thermofisher.com/de/de/home.html

RESOURCE AVAILABILITY

Lead Contact

Further information and requests for resources and reagents should be directed to and will be fulfilled by the Lead Contact, Martin Scheffner (martin.scheffner@uni-konstanz.de).

Materials Availability

Plasmids generated in this study are available upon request.

Data and Code Availability

The MS data (raw files, *xQuest* and *xTract* search output files) have been deposited to the ProteomeXchange Consortium via the PRIDE partner repository (Perez-Riverol et al., 2019) with the dataset identifier PRIDE: PXD020602 (Username: reviewer40058@ebi.ac.uk, Password: Xubb6LPf).

EXPERIMENTAL MODEL AND SUBJECT DETAILS

Bacterial cells (*E. coli* Rosetta 2(DE3), *E. coli* BL21 (DE3), *E. coli* pLysS, *E. coli* XL-10 gold) were grown at 37°C and continuous shaking at 180 rpm in LB medium containing appropriate antibiotics. High Five insect cells (BTI-TN-5B1-4) were grown in 10 cm cell culture dishes at 27°C in TC-100 insect medium supplemented with 10% FCS and 50 mg/L Gentamycin. H1299 cells and H1299-K3 cells, in which endogenous E6AP expression is stably down-regulated by RNA interference (Kuballa et al., 2007), were cultivated in 10 cm cell culture dishes at 37°C, 95% humidity, and 5% CO_2 in 4.5 g/L D-Glucose, L-Glutamine, pyruvate-free DMEM supplemented with 10% FCS. Cell lines have recently not been authenticated.

METHOD DETAILS

Site-Directed Mutagenesis

To introduce point mutations into E6AP bacterial expression vector PCR-based Quick-change site-directed mutagenesis was carried out with PFU Turbo polymerase (Agilent) and overlapping primers harboring the desired nucleotide mutations. Subsequent DpnI (NEB) digest of template DNA was performed according to the manufacturer's instructions prior to transformation in super-competent *E. coli* XL-10 gold cells.

Expression and Purification of His-E6AP

N-terminally His-tagged wild-type E6AP (isoform 1 (Yamamoto et al., 1997)) as well as AS-derived E6AP variants were expressed in *E. coli* Rosetta 2(DE3) cells. At OD_{600} of about 0.6, expression of E6AP was induced by addition of 500 μM IPTG, and cells were cultured at 20°C overnight. Upon centrifugation, cell pellets derived from 1 L bacterial culture were resuspended in 50 mL lysis buffer (25 mM Tris-HCl, 50 mM NaCl, 0.1% Triton-X 100, 1 mM DTT, 1 μg/mL Aprotinin, 1 μg/mL Leupeptin, 100 μM Pefabloc, pH 7.5), sonicated, and centrifuged (30,000 x g, 4°C, 15 min). The supernatant was applied to a Nickel-NTA chromatography column (5 mL HisTrap FF crude column (GE Healthcare)), washed with 8 column volumes of 96% buffer A and 4% buffer B, and bound proteins were eluted with a gradient to 100% buffer B in 20 column volumes (buffer A: 25 mM Tris-HCl, 50 mM NaCl, 1 mM DTT, pH 7.5; buffer B: 25 mM Tris-HCl, 50 mM NaCl, 1 mM DTT, 500 mM imidazole, pH 7.5). Fractions containing E6AP were pooled and subjected to a second purification step via anion-exchange chromatography (1 mL HiTrap Q HP column (GE Healthcare)) with a gradient from 0 to 50% buffer B in 20 column volumes (buffer A: 25 mM Tris-HCl, 50 mM NaCl, 1 mM DTT, pH 7.5; buffer B: 25 mM Tris-HCl, 1 M NaCl, 1 mM DTT, pH 7.5). Elution fractions containing E6AP were pooled and subjected to buffer exchange (25 mM Tris-HCl, 50 mM NaCl, 1 mM DTT, pH 7.5) using 4 mL Amicon Ultra Centrifugal Units with a cut-off of 30 kDa (Millipore). Concentration was adjusted to 100 ng/μL in storage buffer (25 mM Tris-HCl, 50 mM NaCl, 10% glycerol, 1 mM DTT, 1 μg/mL Aprotinin, 1 μg/mL Leupeptin, 100 μM Pefabloc, pH 7.5), and aliquots were stored at - 80°C.

Expression and Purification of E6AP_HECT

N-terminally His-tagged HECT domain of E6AP (E6AP_HECT; amino acid residues 500-852; numbering according to (Yamamoto et al., 1997)) was expressed in *E. coli* Rosetta 2(DE3) cells. At OD_{600} of about 0.6, protein expression was induced by 500 μM IPTG and cells were cultured at 20°C overnight. Pellets derived from 1 L bacterial culture were resuspended in 50 mL lysis buffer (25 mM Tris-HCl, 50 mM NaCl, 0.1% Triton X-100, 1 mM DTT, 1 μg/mL Aprotinin, 1 μg/mL Leupeptin, 100 μM Pefabloc, pH 7.5), sonicated, and centrifuged (30,000 x g, 4°C, 15 min). The supernatant was subjected to Nickel-NTA chromatography as described above for full-length E6AP. Fractions containing E6AP_HECT were pooled and dialyzed against 2 L dialysis buffer (25 mM Tris-HCl, 50 mM NaCl, 0.2 mM DTT, pH 7.5). The dialyzed protein solution was adjusted to 100 ng/μL, containing 1 μg/mL Aprotinin, 1 μg/mL Leupeptin, 100 μM Pefabloc, 1 mM DTT. The purified protein was stored in aliquots at - 80°C.

Expression and Purification of GST Fusion Proteins

GST fusion proteins of HPV-16 E6, HDM2_RING, RLIM_RING, and HUWE1_trunc (amino acid residues 3474-4374) were expressed in *E. coli* BL21 (DE3) pLysS cells. At OD_{600} of about 0.6, protein expression was induced by addition of 500 μM IPTG and cells were cultured at 20°C overnight. Upon centrifugation, cell pellets derived from 1 L bacterial culture were resuspended in 50 mL lysis buffer (PBS, 1% Triton X-100, 1 mM DTT, 1 μg/mL Aprotinin, 1 μg/mL Leupeptin, 100 μM Pefabloc), sonicated and centrifuged with 30,000 x g at 4°C for 15 min. The supernatant was added to 150 μL Glutathione Sepharose beads (GE Healthcare) pre-equilibrated in lysis buffer. Upon incubation for 90 min at 4°C in a tube roller incubator, beads were spun down, washed with 3x 1 mL washing buffer (PBS, 0.1% Triton X-100, 1 mM DTT), and the protein of interest was eluted with 6x 500 μL elution buffer (25 mM Tris-HCl, 10 mM glutathione, 1 mM DTT, pH 8.0).

Expression and Purification of E1

For E1 (UBA1) expression, confluent High Five insect cells were resuspended and plated on a 10 cm dish to 60% confluency. After 90 min, medium was exchanged, and 200 μL E1 baculovirus stock solution was added to each dish. After 44 h incubation at 27°C, cells were harvested and washed with PBS. Next, they were resuspended in TNN lysis buffer (100 mM Tris-HCl, 100 mM NaCl, 1% NP40, 1 μg/mL Aprotinin, 1 μg/mL Leupeptin, 100 μM Pefabloc, 1 mM DTT, pH 8.0) and incubated on ice for 90 min. For lysate derived from one 10 cm plate, 100 μL Q-Sepharose beads (GE Healthcare) were packed in a gravity-flow column and equilibrated with 20 mL wash buffer (25 mM Tris-HCl, 125 mM NaCl, pH 7.4). The lysate was cleared by centrifugation (20 min, 4°C, 30,000 x g), and the supernatant was loaded onto the beads. Beads were washed with 25 mL wash buffer (25 mM Tris-HCl, 125 mM NaCl, pH 7.4), and E1 was eluted in 1 mL fractions with elution buffer (25 mM Tris-HCl, 300 mM NaCl, 1 μg/mL Aprotinin, 1 μg/mL Leupeptin, 100 μM Pefabloc, 1 mM DTT, pH 7.4). Fractions containing E1 were pooled and diluted with buffer (25 mM Tris-HCl, 25 mM NaCl, 1 mM DTT, pH 7.4) to 100 ng/μL. E1 was stored in aliquots at - 80°C.

Expression and Purification of E2 Enzymes

C-terminally His-tagged UbcH5b and UbcH7 were expressed in *E. coli* BL21 (DE3) cells. Cells were grown to an OD_{600} of about 0.6, and upon induction of expression by addition of 500 μM IPTG cells were cultured at 37°C for an additional 5 h. Cells from 500 mL bacterial culture were pelleted by centrifugation and resuspended in 10 mL lysis buffer (PBS, 1% Triton X-100, 10 mM imidazole, 1 mM DTT, 1 μg/mL Aprotinin, 1 μg/mL Leupeptin, 100 μM Pefabloc). After 10 min incubation on ice, cells were sonicated and centrifuged (15 min, 30,000 x g, 4°C). The supernatant was incubated with 1 mL Ni-NTA beads pre-equilibrated in lysis buffer. After 1 h incubation at 4°C, beads were spun down, washed with 15 mL wash buffer 1 (PBS, 0.1% Triton X-100) and then with 20 mL wash buffer 2 (PBS, 0.1% Triton X-100, 1 mM DTT, 50 mM imidazole). Then, beads were resuspended in 10 mL wash buffer 3 (25 mM Tris-HCl, 300 mM NaCl, 0.1% Triton X-100, 1 mM DTT, 50 mM imidazole, pH 7.5) and loaded onto a gravity-flow column. Beads were washed with 10 mL wash buffer 3 and eluted with 6 x 1 mL elution buffer (25 mM Tris-HCl, 300 mM NaCl, 1 mM DTT, 250 mM imidazole, 1 μg/mL Aprotinin, 1 μg/mL Leupeptin, 100 μM Pefabloc, pH 7.5). E2 containing fractions were pooled

and dialyzed against 2 L of dialysis buffer (25 mM Tris-HCl, 300 mM NaCl, 0.2 mM DTT, 5% glycerol, pH 7.5). The dialyzed protein solution was diluted with storage buffer (25 mM Tris-HCl, 100 mM NaCl, 5% glycerol, 1 mM DTT, 1 μg/mL Aprotinin, 1 μg/mL Leupeptin, 100 μM Pefabloc, pH 7.5) to 100 ng/μL and the E2s stored in aliquots at - 80°C.

Expression and Purification of UbLIA

The ubiquitin mutant UbLIA (substitution of L8 and I44 by A) (Mortensen et al., 2015) was expressed in *E. coli* BL21 (DE3) cells. After induction with 500 μM IPTG at OD_{600} of about 0.6, cells were cultured at 37°C for 5 h. Pellets from 1 L bacterial culture were resuspended in 20 mL lysis buffer (25 mM Tris-HCl, 50 mM NaCl, 1 μg/mL Aprotinin, 1 μg/mL Leupeptin, 100 μM Pefabloc, 1 mM DTT). The solution was sonicated and centrifuged for 15 min at 4°C and 30,000 x g. The supernatant was heated to 70°C for 20 min and then centrifuged with 30,000 x g. Next, UbLIA was further purified via ion-exchange chromatography using a 1 mL HiTrap SP HP column (GE Healthcare) and size exclusion chromatography using a HiLoad 26/60 Superdex75 prep grade column (GE Healthcare) with an ÄKTA pure 25 system (GE Healthcare).

TAMRA-Labeling of Ubiquitin

In order to attach the fluorescent dye 5(6)-Carboxytetramethylrhodamine (TAMRA) to ubiquitin, ubiquitin from bovine erythrocytes (Sigma-Aldrich) was dissolved in 50 mM NaOAc (pH 7.2) and incubated for 30 min at 4°C. TAMRA-NHS (Invitrogen) was freshly dissolved in DMSO and added to ubiquitin in a molar ratio of 1:3. The final reaction concentrations were 3 mg/mL ubiquitin, 0.55 mg/mL TAMRA-NHS, and 10% DMSO (v/v). After overnight incubation at 4°C, the reaction was quenched with 50 mM Tris-HCl (pH 8.0) for 30 min at 30°C. 30 mL of 25 mM NaOAc (pH 4.0) were added, pH was adjusted to 4.0, and the solution was filtrated through a 0.22 μm syringe filter. Ub-T (ubiquitin labeled with TAMRA) was further purified via ion exchange chromatography using a 1 mL HiTrap SP HP column (GE Healthcare) with a gradient of 20 column volumes from 0% buffer B to 100% buffer B (buffer A: 25 mM NaOAc, pH 4.0; buffer B: 25 mM NaOAc, 1 M NaCl, pH 4.0) on an ÄKTA pure 25 system (GE Healthcare). 4 mL Amicon filter devices with a cut-off of 10 kDa (Millipore) were used for further purification and buffer exchange to storage buffer (25 mM Tris-HCl, 50 mM NaCl, 1 mM DTT, pH 7.5). Purified Ub-T was stored at -80°C.

Analysis of TAMRA-Labeled Ubiquitin (Ub-T)

Ub-T was analyzed by UHPLC on a Dionex UltiMate3000 (Thermo Fisher) using an analytical Aeris WIDEPORE XB-C8 column (150 mm x 2.1 mm) with 3.6 μm silica as stationary phase (Phenomenex). Prior to purification, all samples were acidified with 0.1% TFA. Gradient elution (2 min at 0% B; in 38 min to 70% B; then in 7 min to 100% B, and finally for 5 min at 100% B) with eluent A (0.04% TFA in water) and eluent B (0.04% TFA in acetonitrile/water (80:20, v/v)) was performed at a flow rate of 250 μl/min. The signals were monitored by UV absorbance at 220 nm.

Ub-T was further analyzed by MALDI-TOF mass spectrometry with a MicroFlex MALDI-TOF instrument (Bruker). 1 μL α-cyano-4-hydroxycinnamic acid (HCCA) was spotted as matrix on the sample target chip. 2 μL sample solution (2 μg/μL) was mixed with the matrix. After drying, samples were measured. The instrument was calibrated with commercially available protein standards from Bruker.

To identify TAMRA modification site(s) on ubiquitin, LC-MS/MS measurements were performed. Ub-T preparations were subjected to SDS-PAGE; respective bands were cut out, stored in 50 mM NH_4HCO_3, destained with acetonitrile/NH_4HCO_3 (1:1, v/v) solution and dried in acetonitrile. After washing twice for 5 min with acetonitrile/NH_4HCO_3 (1:1, v/v) solution, samples were stored in 1 mM DTT at 4°C. Later, gel pieces were dried with acetonitrile and covered with 10 μg/mL trypsin solution in 50 mM NH_4HCO_3 for 1 h at 4°C. After removing the supernatant, proteins were in-gel digested at 30°C overnight. On the next day, peptides were eluted with 0.1% formic acid for 1 h at 4°C. Peptides were desalted and concentrated using C18-ZipTips (Millipore) according to the manufacturer's instructions. Digested samples were analyzed by reversed phase liquid chromatography nanospray tandem mass spectrometry (LC-MS/MS) using an LTQ-Orbitrap mass spectrometer (Thermo Fisher) and an Easy-nLC 1000 (Thermo Fisher). The dimensions of the reversed-phase LC column were 3 μm, 100 Å pore size C18 resin in a 75 μm i.d. × 15 cm long piece of fused silica capillary (Acclaim PepMap100, Thermo Scientific). After sample injection, the column was washed for 5 min with 94% mobile phase A (0.1% formic acid) and 6% mobile phase B (0.1% formic acid in acetonitrile), and peptides were eluted using a linear gradient of 6% mobile phase B to 36% mobile phase B in 45 min, then to 100% B in an additional 5 min, at 300 nL/min. The LTQ-Orbitrap mass spectrometer was operated in a data-dependent mode in which each full MS scan (30,000 resolving power) was followed by five MS/MS scans where the five most abundant molecular ions were dynamically selected and fragmented by collision-induced dissociation (CID) using a normalized collision energy of 35% in the LTQ ion trap. Dynamic exclusion was allowed. Tandem mass spectra were searched against a StandardProt database using Proteome Discoverer 1.4 (Thermo Scientific) and an in-house Mascot Server 2.5 (Matrix Science) with "Trypsin/P" enzyme cleavage, static cysteine alkylation by chloroacetamide and variable methionine oxidation as well as variable TAMRA modification at lysine residues.

FP-Based *In Vitro* Ubiquitination Assay

FP-based *in vitro* ubiquitination assays were performed in 384 well plates (Greiner BIO-ONE, PS, flat bottom, black, non-binding) in a total volume of 80 μL. Reactions were started by addition of 20 μL premix 2 containing E1, E2, non-modified ubiquitin, and Ub-T to 60 μL premix 1 containing ATP and E6AP. When not indicated differently, final concentrations of components were: 3 nM E1, 25 nM E2 (UbcH5b or UbcH7), 12 nM E6AP, 230 nM ubiquitin, 23 nM Ub-T in 25 mM Tris-HCl, 50 mM NaCl, 0.01% Triton X-100, 0.5 mM

ATP, 2 mM $MgCl_2$, 1 mM DTT. Plates were incubated at 30°C and fluorescence polarization was measured using an Infinite F500 microplate reader (Tecan). Alternatively, samples were subjected to SDS-PAGE. Gels were scanned with a FLA-5000 (Fujifilm) using 532 nm laser excitation and 575 nm (LPG) emission filter with 800 V detection mode.

High-throughput Screening

For high-throughput screening (HTS), the FP-based *in vitro* ubiquitination assay was used. For automation, assays were carried out by an EVO Freedom HTS workstation (Tecan). The room temperature was constantly kept at 22°C using air conditioning, and premixes 1 and 2 were stored in open vessels at 4°C during one run with 10 to 20 384 well plates (every 28 min the reactions in one plate were started). HTS was performed with 12 nM E6AP, and positive controls contained additionally 15 nM of GST-16 E6. Compounds were transferred from 10 mM libraries to a final concentration of 50 μM. E6AP was preincubated with the compounds at 30°C by shaking at 500 rpm for 20 minutes. Upon reaction start, FP was measured at 0, 45, and 55 min with prior 10 sec plate shaking. In total, 48077 compounds from commercially available libraries (Maybridge HitKit9000, ChemBioNet 1-3, ChemDiv, Analyticon Discovery I (1000 natural compounds), Analyticon Discovery II (5000 semi-natural compounds) and Biomol ICCB (480 FDA approved drugs with known targets)) were screened. Additionally, 686 small molecules from an in-house library (named MDB) were screened with an assay concentration of 12.5 μM. Screening data were evaluated using KNIME (Konstanz Information Miner) software (Berthold et al., 2008).

EC50 Determination

For EC50 determination, FP-based E6AP autoubiquitination assays were performed as described above with 50 nM, 167 nM, 500 nM, 1.67 μM, 5 μM, 16.7 μM, and 50 μM of the respective compounds. FP values at 55 min were used to determine EC50 concentrations by non-linear regression (fitting with a variable slope with four parameter logistic) with GraphPad Prism.

In Vitro Auto-ubiquitination Assay

In vitro auto-ubiquitination assays were performed in 30 μL volumes as described previously (Nuber et al., 1998). The assay mixture contained 50 nM E1, 150 nM E2, 250 nM E6AP, 7.8 μM ubiquitin in reaction buffer (25 mM Tris-HCl, 50 mM NaCl, 2 mM ATP, 2 mM $MgCl_2$, 2 mM DTT, pH 7.5) and was incubated for 90 min or indicated times at 30°C. Reactions were stopped by addition of 7.5 μL 5x stop buffer (312.5 mM Tris-HCl (pH 6.8), 500 mM DTT, 10% SDS, 0.001% bromophenol blue) and boiling for 5 min. Proteins were separated by electrophoresis in a 12% SDS-PA gel and detected by Coomassie blue staining.

In Vitro Ubiquitination of Ring1B_I53S

HA-tagged Ring1B_I53S (Mortensen et al., 2015; Zaaroor-Regev et al., 2010) was *in vitro* translated in the presence of ^{35}S-labeled methionine using the T7-coupled TNT *in vitro* reticulocyte lysate translation system (Promega) according to the manufacturer's instructions. Upon translation, HA-Ring1B_I53S was purified with E/Z view α-HA agarose beads (Sigma-Aldrich). For purification, beads were washed twice with 500 μL wash buffer (25 mM Tris-HCl pH 7.5, 50 mM NaCl). For each ubiquitination reaction, 1 μL bead slurry was incubated with 1 μL *in vitro* translation reaction by shaking at 1000 rpm for 1 h at 4°C. Then, beads were washed 3 times with 500 μL wash buffer. *In vitro* ubiquitination assays were performed in 30 μL volumes with an assay mixture containing 50 nM E1, 150 nM E2, 100 nM E6AP, 40 μM ubiquitin and 1 μL on beads immobilized radiolabeled HA-Ring1B_I53S in reaction buffer (25 mM Tris-HCl pH 7.5, 50 mM NaCl, 2 mM ATP, 2 mM $MgCl_2$, 2 mM DTT). The reaction mixtures were incubated at 30°C for 90 min or the times indicated, and reactions were stopped by adding 7.5 μL 5x stop buffer (312.5 mM Tris-HCl pH 6.8, 500 mM DTT, 10% SDS, 0.001% bromophenol blue) and boiling for 5 min. Proteins were separated by electrophoresis on a 12% SDS-PA gel. The gel was subsequently fixed for 30 min in fixing solution (10% acetic acid, 40% methanol, MilliQ) and subsequently incubated in Lightning Autoradiography Enhancer solution (PerkinElmer). Gels were vacuum-dried at 80°C, subjected to a BAS MS-2040 imaging plate (Fujifilm), and signals were read out by a FLA-5000 scanner (Fujifilm).

Ubiquitin Thioester Complex Formation Assay

To determine the ability of AS-derived E6AP variants to form thioester complexes with ubiquitin, 200 nM E1, 3.75 μM UbcH7, and 375 nM E6AP were incubated with 15 μM ubiquitin and 1.1 μM Ub-T for 0, 1, 2 and 5 min at 30°C in 20 μL volumes. In addition, reactions contained 25 mM Tris-HCl pH 7.5, 50 mM NaCl, 0.1 mM DTT, 2 mM ATP, and 10 mM $MgCl_2$. Reactions were terminated by incubating the mixtures for 15 min at 30°C in urea loading buffer (2x urea loading buffer: 8 M urea, 0.1 M Tris-HCl pH 6.8, 10% Glycerol, 4% SDS, 0.001% bromophenol blue) or urea loading buffer containing 25 mM DTT (reducing conditions). Whole reaction mixtures were separated on 7.5-15% SDS-PA gradient gels at 4°C and analyzed by fluorescence scan.

Degradation of Ectopically Expressed Ring1B_I53S

H1299-K3 cells were seeded in 6-well tissue culture plates. At 80-90% confluency, cells were transiently transfected using Lipofectamin 2000 (Thermo Fisher Scientific) according to the manufacturer's instructions. After 5 h, medium was exchanged with fresh medium containing the compounds indicated or an equal volume of DMSO. After 16 h, cells were washed twice with ice-cold PBS and harvested by scraping. After centrifugation, cells were lysed for 30 min at 4°C with 90 μL TNN buffer (100 mM Tris-HCl, 100 mM NaCl, 1% NP40, 1 μg/mL Aprotinin, 1 μg/mL Leupeptin, 100 μM Pefabloc, 1 mM DTT, pH 8.0) and then cleared by centrifugation (30 min, 4°C, 16,000 x g). The amounts of lysates used for Western blot analysis were adjusted prior to SDS-PAGE based on

β-galactosidase activity (a respective expression construct was co-transfected in all transfections). Upon Western blot analysis with an anti-HA antibody, band intensities were determined with AIDA image analysis software (Elysia-Raytest).

Cytotoxicity Assay

H1299 cells or H1299-K3 cells were suspended in cell culture medium and counted with a COUNTess automated cell counter (Thermo Fisher). 50,000 cells were seeded in 500 μL DMEM in 24 well tissue culture plates. After 20 h, DMEM was exchanged with DMEM containing compounds in the indicated concentrations. After 24 h, cells were washed twice with ice-cold PBS and stained with 500 μL crystal violet (0.1% w/v)/formaldehyde (4% v/v) solution. After 20 min incubation on a rocking incubator, cells were washed carefully with water and dried at room temperature. Pictures were taken with LAS-3000 imager (FujiFilm).

qXL-MS Analysis

Experiments were carried out essentially as described (Sailer et al., 2018). In short, approximately 100 μg of E6AP or the AS-derived E6AP variants F583S and E584Q were crosslinked by addition of H12/D12 DSS (Creative Molecules) at a ratio of 1.5 nmol/1 μg protein and gentle shaking for 30 min at 37°C. Samples contained either 100 μM of OF232, alloxazine or an equal volume of DMSO (1% v/v). After addition of the compounds or DMSO, samples were incubated for 30 min on ice prior to crosslinking. In order to crosslink E6AP in complex with HPV-16 E6, a 1.5-fold molar excess of GST-16 E6 to E6AP was used and incubated and crosslinked under the same conditions. Proteins were crosslinked directly after purification without freezing. After quenching by addition of ammonium bicarbonate to a final concentration of 50 mM, samples were reduced, alkylated, and digested with trypsin. The resulting peptides were separated from the solution by a solid phase extraction system (SepPak, Waters), and then crosslinked peptides were enriched by size exclusion chromatography prior to liquid chromatography (LC)-MS/MS analysis on an Orbitrap Fusion Tribrid mass spectrometer (Thermo Scientific). MS measurement was performed in data-dependent acquisition mode with a cycle time of 3 s. The full scan was done in the Orbitrap with a resolution of 120,000, a scan range of 400-1500 m/z, AGC Target 2.0e5 and injection time of 50 ms. Monoisotopic precursor selection and dynamic exclusion was used for precursor selection. Only precursor charge states of 3-8 were selected for fragmentation by CID using 35% activation energy. MS2 was carried out in the Ion Trap in normal scan range mode, AGC target 1.0e4 and injection time of 35 ms. Data were searched using *xQuest* (Leitner et al., 2014) in ion-tag mode with a precursor mass tolerance of 10 ppm. For matching of fragment ions, tolerances of 0.2 Da for common ions and 0.3 Da for crosslink ions were applied. Crosslinked samples were prepared in biological triplicates (i.e. separately expressed and purified batches of proteins) for all investigated samples, and each of these was measured with technical duplicates. Crosslinks were only considered during structural analysis, if they were identified in at least 2 of 3 biological replicates with deltaS < 0.95 and at least one Id score $\geq$25.

For quantitative XL-MS analysis, the chromatographic peaks of identified crosslinks were integrated and summed up over different peak groups (taking different charge states and different unique crosslinked peptides for one unique crosslinking site into account) for quantification by *xTract* (Walzthoeni et al., 2015). Amounts of potential crosslinks were normalized prior to MS by measuring peptide bond absorption at 215 nm for each fraction. Only high-confidence crosslinks that were identified consistently over different biological and technical replicates in a peak group (*xTract* settings violations was set to 0) were selected for further quantitative analysis. Changes in crosslinking abundance are expressed as $\log_2$ ratio (e.g. abundance state 1 was quantified versus abundance state 2). The *p*-value using a two-sided t-test indicates the regression between the two conditions. Thus, in this study, only changes that showed at least a change of log2ratio $\geq \pm 1.0$ and a p-value of ≤ 0.01 were considered significant changes in abundance and are shown in green ($\log_2$ratio ≥ 1) and red ($\log_2$ratio ≤ 1) in the 2D visualizations, respectively. All other changes were considered insignificant and are shown in grey.

A list of all identified and quantified links can be found in Data S1.

QUANTIFICATION AND STATISTICAL ANALYSIS

FP-based ubiquitination assays were evaluated with GraphPad Prism 6 software with error bars indicating SD of three technical replicates. E1 activity assays (Figure S3D) were also evaluated with GraphPad Prism 6. Data were normalized to reaction in the absence of E1 with error bars indicating SEM of three technical replicates.